THE GUT BRAIN AXIS: IMPACT OF DIETARY FIBER ON A MURINE MODEL OF MULTIPLE SCLEROSIS

by

Hannah Robinson

B.Sc., The University of California, Santa Barbara, 2016

A THESIS SUBMITTED IN PARTIAL FULFILLMENT OF

THE REQUIREMENTS FOR THE DEGREE OF

MASTER OF SCIENCE

in

THE FACULTY OF GRADUATE AND POSTDOCTORAL STUDIES

(Microbiology and Immunology)

THE UNIVERSITY OF BRITISH COLUMBIA

(Vancouver)

April 2019

The following individuals certify that they have read, and recommend to the Faculty of Graduate and Postdoctoral Studies for acceptance, a thesis/dissertation entitled:

The Gut Brain Axis: Impact of Dietary Fibers on a Murine Model of Multiple Sclerosis

submitted by Hannah Robinson in partial fulfillment of the requirements for

the degree of Master of Science

in Microbiology and Immunology

Examining Committee:

Dr. Lisa Osborne
Supervisor

Dr. Marc Horwitz
Supervisory Committee Member

Dr. Sean Crowe
Supervisory Committee Member

Additional Examiner

Additional Supervisory Committee Members:

Supervisory Committee Member

Supervisory Committee Member

Abstract

Multiple Sclerosis (MS) is a chronic autoimmune disease of the central nervous system (CNS) that causes demyelination of neurons, neurodegeneration and progressive disability. The exact cause of Multiple Sclerosis remains unknown however, susceptibility to MS is influenced by genetics and environmental factors, such as diet. As zero-fiber diets have been associated with exacerbated disease in inflammatory disease models, we investigated dietary fiber's impact on the murine model of MS, experimental autoimmune encephalomyelitis (EAE). We demonstrated that standard fiber diets (5%) do not offer protection against EAE when compared to zero-fiber diets, whereas a diet high in the soluble fiber, guar gum (30%), inhibited disease progression and prevented lymphocytic CNS infiltration. Other soluble fibers: pectin, resistant starch and inulin did not offer the same protection – providing evidence that the types of dietary fiber have differential effects on the immune system and neuroinflammation.

Lay Summary

Dietary fiber, a key dietary component that is indigestible by humans, is processed by microbes living in our intestine. Microbial digestion of fiber leads to production of molecules that have been shown to promote the development and/or function of anti-inflammatory immune cells. Furthermore, dietary fiber has been linked to beneficial roles in a variety of inflammatory diseases, however its role in multiple sclerosis (MS) – an autoimmune disease which results in neurodegeneration of the central nervous system (CNS) – remains unknown. I investigated whether a zero-fiber diet would exacerbate disease in a murine model of MS and no differences were observed in severity of disease. However, when I used a diet that contained supraphysiological amounts of the dietary fiber guar gum, it was observed that guar gum offered protection from paralysis and immune cell infiltration into the CNS. Therefore, fiber's role – specifically guar gums – in disease in MS patients should be investigated.

Preface

All experimental protocols were approved by the Animal Care Committee of UBC (A15-0122 and A17-0037) and experiments performed in accordance with guidelines set by Canadian Council for Animal Care. Biosafety protocol B15-0113 was approved by UBC's Biosafety Committee.

Figures from Chapter 1 were modified from a literature review in preparation for submission: *Impact of environmental influences on the microbiome and autoimmune neuroinflammation* by HG Robinson, NM Fettig & LC Osborne. A version of Figures 3.1-3.7 from Chapter 3 were modified from a primary research article in preparation for submission: Impact of Dietary Soluble Fiber on Autoimmune Neuroinflammation by HG Robinson, R Simister, JR Allanach, AJ Sharon, BK Hardman, NM Fettig, N Saleh, K Doshi, S Crowley, BA Vallance, MS Horwitz, S Crowe & LC Osborne. I will be primary author and will write the manuscripts. For the research article, I conceived of the project with LC Osborne and conducted data collection and analysis for all *in vivo* experiments, with technical support from JR Allanach, AJ Sharon, BK Hardman, NM Fettig and N Saleh. Sample preparation was performed by R Simister and sequenced at the Pharmacological Sciences core facilities at UBC. Sequence analysis was performed by R Simister, K Doshi and myself. S Crowley and BA Vallance provided technical expertise for analysis of colonic mucus widths.

Table of Contents

List of Tables

List of Figures

List of Symbols

α	Alpha
β	Beta
γ	Gamma
μ	Micron
%	Percent
I	One
II	Two

List of Abbreviations

ACC	Animal care committee
ACK	Ammonium-Chloride-Potassium
BBB	Blood brain barrier
BFA	Brefeldin A
B_{REG}	Regulatory B cell
CD	Cluster of differentiation
cDNA	Complementary deoxyribonucleic acid
CFA	Complete Freud's adjuvant
CDM	Center for Disease Modeling
CHS	Clinical health score
CNS	Central nervous system
CTL	Cytotoxic T lymphocyte
DC	Dendritic cell
DNA	Deoxyribonucleic acid
DMEM	Dulbecco's Modified Eagle Medium
EAE	Experimental autoimmune encephalomyelitis
EDTA	Ethylenediaminetetraacetic acid
ELISA	Enzyme-linked immunosorbent assay
FACS	Flow cytometry
FBS	Fetal bovine serum
FcR	Fc receptor
FITC	Fluorescein Isothiocyanate

Fp	Fecal pellet
Foxp3	Forkhead box P3
GM-CSF	Granulocyte-macrophage colony-stimulating factor
GPR	G-coupled protein receptor
HEPES	Hydroxyethyl piperazineethanesulfonic acid
HLA	Human Leukocyte Antigen
IFA	Incomplete Freud's adjuvant
IFN	Interferon
Ig	Immunoglobulin
IL	Interlukin
LCFA	Long chain fatty acid
LFA	Lymphocyte function-associated antigen
Ly6C	Lymphocyte Ag 6C
Ly6G	lymphocyte Ag 6G
M1	Pro-inflammatory macrophage
M2	Anti-inflammatory macrophage
MAPK14	Mitogen-activated protein kinase 14
MBF	Modified Barrier Facility
MCP	Monocyte chemoattractant protein
MFI	Mean fluorescence intensity
MHC	Major histocompatibility complex
MHI	Mental health inventory
MIP	Macrophage inflammatory protein

MNV	Murine norovirus
MOG	Myelin oligodendrocyte glycoprotein
MS	Multiple sclerosis
NCS	Neo-natal calf serum
NK	Natural killer
PBS	Phosphate buffered saline
PB	Pacific blue
PE-Cy7	Phycoerythrin-Cyanine7
PE	Phycoerythrin
PCS	Physical component summary
PGE	Prostaglandin E
PMA	Phorbol 12-myristate 13-acetate
RPMI	Roswell Park Memorial Institute
RNA	Ribonucleic acid
RRMS	Relapse-remitting multiple sclerosis
SCFA	Short chain fatty acid
Sp.	species
SPMS	Secondary progressive multiple sclerosis
TCR	T cell receptor
TGF	Transforming growth factor
T_H1	T helper 1 cell
T_H17	T helper 17 cell
T_H2	T helper 2 cell

TNF	Tumor necrosis factor
T_{REG}	Regulatory T cell
UBC	University of British Columbia
VLA	Very late antigen

Acknowledgements

I'd like to thank the University of British Columbia, facility staff and funding sources for making this research project possible. I owe my gratitude to Dr. Lisa Osborne, whose patience and support made my Master's degree a compelling experience and has inspired me to further my education. I appreciate my committee members Dr. Sean Crowe and Dr. Marc Horwitz, whose feedback has propelled me to be a better scientist. To my lab mates from the Osborne, Horwitz and Crowe lab, thank you for all your help with my experiments – the size of them require a team to complete them and you are the best team that I could have asked for. To my fellow UBC students and friends, I am thankful for your support and community. I will always remember the joyous memories made from softball pitches to adventures in the mountains.

Chapter 1: Introduction

1.1 Multiple Sclerosis

Multiple Sclerosis (MS) is a chronic autoimmune disease characterized by neurodegeneration due to immune-mediated degradation of the myelin sheath surrounding neuronal axons of the central nervous system (CNS). This damage leads to improper neuronal signaling and a various range of motor and/or cognitive side effects, such as impaired balance, vision, learning and long-term memory[1–3]. Relapsing and remitting MS (RRMS) is the most common form of disease and presents as alternating periods of symptoms and remission[4]. A less common form of MS, primary progressive, presents as a continuous increase in symptoms with no remission[5]. RRMS patients can develop secondary progressive MS (SPMS) where periods of remission disappear and neurodegeneration continues without reprieve[6]. Although MS remains incurable, a number of treatment options exist that can limit progression, reduce symptoms and/or increase quality of life for people living with MS. Supporting the hypothesis that MS is an immune-mediated disease, the majority of these treatment options either ablate immune cells or interrupt signaling pathways necessary for immune function.

Susceptibility to MS is influenced by both genetic and environmental factors, including diet, infection history, and geographic location[7–9]. Recently, the gut microbiome, the collection of viruses, archaea, bacteria, fungi and protists that inhabit the intestines has been linked to both disease progression and prevention[10,11]. Multiple studies have observed that adult and pediatric MS patients have microbial dysbiosis[11–13], with certain species similarly reduced in other inflammatory conditions, such as inflammatory bowel disease[14,15]. Although each study concludes that MS patient microbiomes are distinct from healthy controls, there are few

consistencies in the types of microbes that have been found that differ between control and MS subjects. It remains unknown whether these changes are causative or occur in response to disease development. Because the microbiome regulates the immune system[16], these data provoke the hypothesis that microbial community composition and function may alter the immune system and contribute to either MS susceptibility or progression.

1.2 EAE: a murine model of human MS

There are many ways to model neuroinflammation that mimics MS in mice, including experimental autoimmune encephalomyelitis (EAE), coronavirus-induced demyelination disease[17], adoptive T cell transfer[18] (passive disease) and toxic demyelination upon cuprizone administration[19]. These models, along with human studies, indicate that both innate and adaptive immune cell lineages are involved in neurodegeneration. My thesis uses EAE, which induces myelin-specific autoimmunity by administration of myelin-derived peptides or proteins along with an adjuvant and reagents that help bypass the blood brain barrier (BBB)[20,21].

Neuroinflammation in EAE is associated with changes in multiple immune cell types and their functions. The innate immune cells involved in disease include macrophages, dendritic cells and NK cells. Both T and B cells of the adaptive immune system contribute to disease. The common thread between both immune categories is that there are pro-inflammatory and anti-inflammatory versions of these cells that either contribute to the pathogenesis or protection against disease[22,23]. In the following sections, we will investigate these cell types' roles in EAE and Multiple Sclerosis in more detail.

1.3 Immune cells and pathways involved in EAE and MS

1.3.1 B cells

Early studies of the role of immune cells in MS implicated plasma cells (antibody secreting B cells) as major contributors to disease pathogenesis due to autoantibodies found in brain lesions[24] and myelin-specific antibodies present in the cerebral spinal fluid of MS patients[25]. In addition, plasma cells have been shown to induce demyelination via the complement system[26,27] and may contribute to disease via interactions with FcRs on pro-inflammatory microglia[28]. However, recent clinical trials have demonstrated that treatment with Rituximab (α-CD20), a reagent that depletes immature and mature B cells but leaves antibody-producing plasma B cells intact can reduce CNS lesions in MS patients. These data indicate that although some populations of B cells contribute to disease progression, autoantibody-secreting plasma cells are not the prime pathogenic B cell subset in MS[29]. Notably, recent data suggests that IL-10+ plasma cells producing commensal-specific IgA were found in the CNS in the context of neuroinflammation and were associated with protection from disease[30].

Independent of antibody production, B cells influence disease pathogenesis through antigen presentation and cytokine secretion. Using a mouse model where MHCII was deleted specifically in B cells, one study determined that B cell-intrinsic MHCII antigen presentation was essential for a B cell dependent EAE disease progression[31]. Furthermore, B cell subsets have been categorized as either protective or pathogenic, defined by their cytokine secretion profile, where B cells secreting IL-6 or GM-CSF have been shown to be pathogenic[32–34], but secretion of IL-10 or IL-35 is associated with protection[32,35–37] (**Fig 1.1**). A subset of IL-10-producing B cells called regulatory B (B_{REG}) cells are protective in EAE[45].

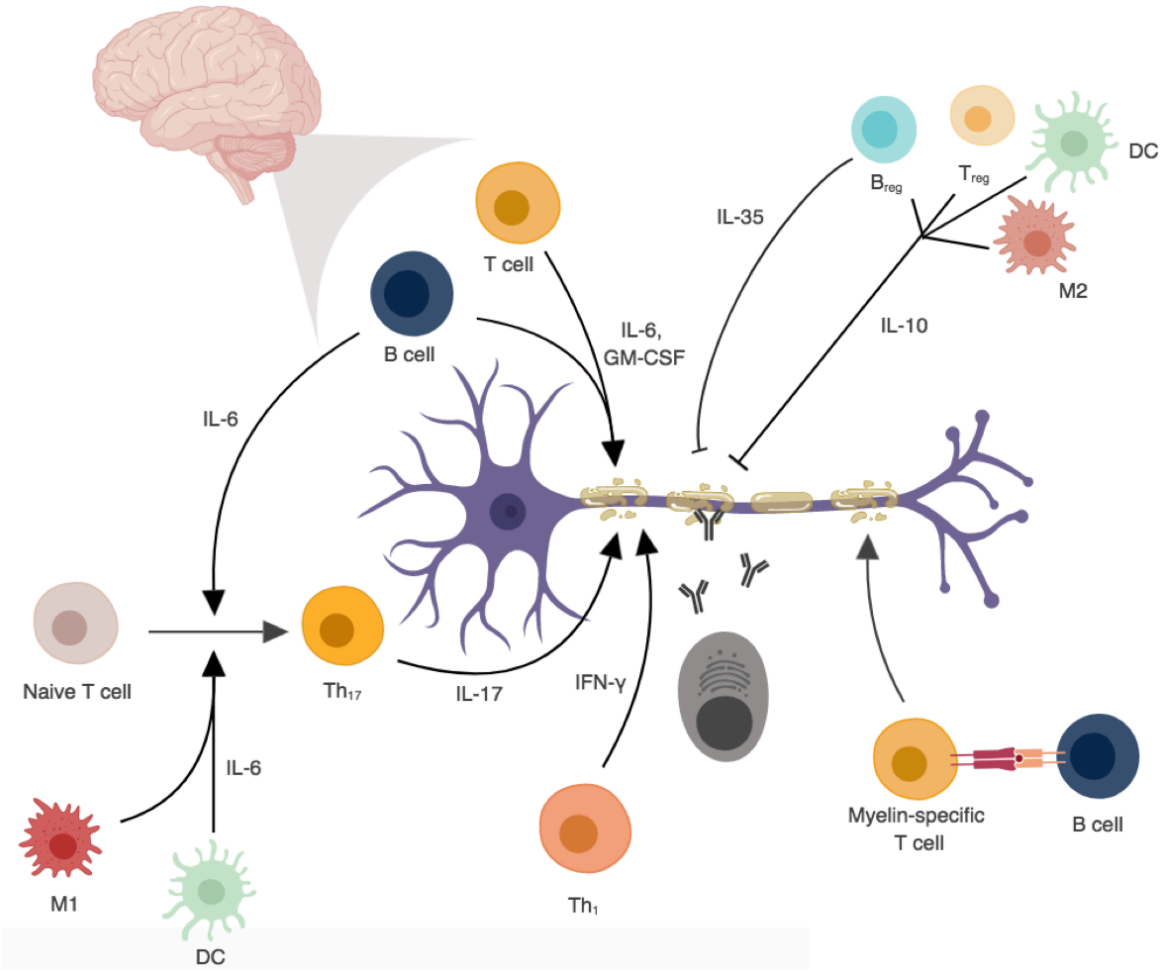

Figure 1.1: Immune cell pathways in the exacerbation and protection against neurodegeneration in murine EAE. Cytokine-mediated influence of B cells, T cells and several innate cells involved in disease pathogenesis. Pro-inflammatory pathways are denoted by arrowheads, anti-inflammatory/myelin-protective pathways are denoted by the inhibitor lines.

1.3.2 T cells

The cell type most commonly associated with EAE and MS are T cells ($CD3^+$ lymphocytes): they are the disease drivers in MOG_{35-55} induced EAE and the cell type used to passively induce EAE. The main T cell subsets that modulate disease pathogenesis in T cell-mediated EAE are $CD4^+$ T helper type 1 (T_H1) cells (identified by IFNγ production), $CD4^+$ T

helper type 17 (T_H17) cells (identified by IL-17 production), and cytotoxic $CD8^+$ T lymphocytes (CTLs)[38–41], which exacerbate disease, and regulatory T cells (T_{REG}) cells (identified by Foxp3 transcription) limit disease severity[44]. Adoptive T cell transfers of myelin specific T_H1 and T_H17 cells have been used to determine the relative contributions of each cell type in the development of EAE[42,43]. Although it remains unclear whether T_H1 cells are sufficient to induce disease, they contribute to the development of neuroinflammation by facilitating the translocation of T_H17 cells across the blood brain barrier in an IFNγ-dependent manner[42–45]. In contrast, T_H17 cell adoptive transfer can consistently initiate disease, suggesting that T_H17 cells are the main T cell subset involved in promoting EAE development. Similarly, in MS, T_H17 cells are consistently elevated in MS patients and are thought to be important contributors to disease progression[46]. The role of T_H1 cells in MS patients remains unclear as one study observed similar amounts in healthy controls[46] but an independent study found that T_H1 cells from MS patients were more likely to be MOG-specific[47,48]. Further, reports of highly inflammatory IFNγ-producing T_H17 cells isolated from MS patients indicate that these cells have reduced gene expression of anti-inflammatory IL-10, which serves to counteract the production and inflammatory effects of IL-6[49]. Along with the toxicity of IL-17 producing T cells, CD8 T cells and GM-CSF expressing helper T cells have been linked to disease pathogenesis in both murine EAE and MS patients[50–54], in which downstream effects of GM-CSF have the potential to regulate of DCs[55] and macrophages[56,57]. T_{REG} cells function as the main T cell subset responsible for reducing the inflammatory effects of effector T cells[58]. Additionally, natural killer T (NK-T) cells have been shown to protect against EAE through dampening T_H1 cell cytokine secretion and shifting the immune system to a T_H2 response[59,60]. MS patients have demonstrated reduced T_{REG} cell function, characterized by a decreased ability to prevent effector cell proliferation *in vitro*[61,62],

indicating that immune dysregulation in MS occurs on both pro-inflammatory and anti-inflammatory fronts.

1.3.3 Macrophages, dendritic and NK cells

Just as adaptive immune cells have dual role in EAE, macrophages/microglia and dendritic cells (DCs) can be proinflammatory mediators of disease and anti-inflammatory inhibitors of disease[63]. The macrophage pro-inflammatory (M1) and anti-inflammatory (M2) phenotypes resemble the DC subsets, determined by cytokine secretion profiles, however the terminology for these DC subsets have yet to be established. DCs contribute to pathogenicity in EAE through antigen presentation and cytokine production. Similar to B cells, CD11c+ DCs play a role in disease pathogenesis through antigen presentation. Using a T cell dependent model, restricting MHCII expression to DCs was sufficient to elicit EAE disease and allow blood-brain barrier penetration. Both B cells and DCs play an integral role in models that rely on different cell types, which cell types more better represent the pathogenesis of neurodegeneration in MS patients is still up for debate[31,64]. Supporting a role for DCs in the initiation of autoimmune neuroinflammation, DCs are known to promote differentiation of T_H17 cells in *vivo* through trans-presentation of IL-6[65]. Furthermore, IL-6 deficient mice were resistant to EAE induction and had decreased numbers of infiltrating macrophages and CNS-resident microglia[66]. Moreover, one study administered the MS drug resveratrol to mice induced with EAE and observed there was a decrease in IL-6 expression in macrophages[67,68], potentially reducing disease via this mechanism. In both DCs and M1 macrophages, IL-6 plays a pivotal role in disease pathogenesis. The homeostasis of M1/M2 cells is important in disease severity – an increased abundance of M1 macrophages promoted paralysis relapses in SJL mice with induced EAE, while M2

macrophages induced recovery[69]. Moreover, IL-10 secreting DCs[70,71], M2 macrophages and microglia can promote remyelination[72,73]. Another innate immune cell type involved in disease are NK cells, which are thought to be protective in EAE, however conflicting data makes their role in disease pathogenesis unclear and an avenue for further exploration[74,75].

Each innate and adaptive immune cell type has a subset analogous to each other in cytokine secretion profiles with similar roles in disease progression. This suggests that the specific cell type has less of an effect on disease than their downstream cytokine production.

1.4 The microbiota in MS

The bacteria that occupy a host's external surfaces, including the skin, gut, lung and urogenital tract – have been linked to susceptibility to inflammatory diseases[76–78]. In MS patients, the relationship between the host microbiota and disease has not been fully uncovered. However, several studies have uncovered that MS patients have altered microbiomes compared to healthy controls[11,12,79,80] (**Table 1.1**). In one study, MS patients' gut microbiomes had altered genera within the following phylums: increased Bacteroidetes: *Pedobacter* and *Flavobacterium*; decreased Bacteroidetes: *Parabacteroides*; increased Firmicutes*: Blautia* and *Dorea;* decreased Actinobacteria: *Adlercreutzia* and *Collinsella*; increased Proteobacteria: *Mycoplana* and *Pseudomonas* and decreased Proteobacteria: *Haemophilus*[12]. In other studies, the genera *Methanobrevibacter* and *Akkermansia* were increased while *Butyricimonas* was reduced in MS patients[11,13]. The inconsistent microbial differences in MS patients across studies could potentially be due to the different locations, diets, sample processing, taxonomic database and other parametes[81,82]. Whether the altered microbial populations in the MS gut microbiome contribute to disease or are a response to a dysregulated immune system remains unknown,

however correlations to other diseases could provide some clues. *Faecalibacterium, Prevotella, Lachnospiraceae,* and *Akkermansia,* which are altered in MS patients, are similarly affected in the neurodegenerative disease, Parkinson's disease. These microbial similarities could suggest that the inflammatory and/or metabolic conditions in Parkinson's and MS patients are similar and lead to an analogous change in the gut ecosystem that allows these bacteria population dynamics to change. Alternatively, it could suggest that people with these microbiome profiles predispose them to either condition. Evidence for the latter is that *Akkermansia* (and *Methanobrevibacter*) was positively correlated with a gene associated with neuronal apoptosis in Parkinson's disease (MAPK14) , whereas *Butyricimonas* was negatively associated[11,83]. Despite microbial consistencies between Parkinson's disease and MS, their compositions of *Blautia*, *Dorea* and *Ruminococcaceae* differ. While the significance of the microbiome in MS remains unclear, its role in EAE is better established – in broad-spectrum oral antibiotic treated and germ-free conditions, mice were resistant to EAE development and autoimmune demyelination was significantly reduced[84–86].

Microbe	**Population change in RRMS patients**	**Immunological Implications**	**Associations in other diseases**
Pedobacter	Increased	----	Increased in Vitamin D cell receptor knock out mice[87] Increased in children with Autism[88] Reduced in colorectal cancer patients[89]
Mycoplana	Increased	----	----
Blautia	Increased	Butyrate (T_{reg} and M2 inducer) producing microbe in mice[16,90,91].	Increase in *Blautia hydrogenotorophica* and a decrease in *Blautia wexlerae* in obese patients[92] Genera and species *Blautia glucerasea* decreased in Parkinson's patients[93,94] Decreased in children with autism[88] Decreased *Blautia hansenii* in Crohn's disease patients[95]
Dorea	Increased	----	Increased in *Trichuris suis* infection[96] Decreased in Parkinson's patients[93,94] Reduced in patients with food sensitization[97]
Pseudomonas	Increased	----	Increased in children with Autism[98]
Methanobrevibacter	Increased	----	*Methanobrevibacter smithii* decreased in obesity, increased in anorexia[99]

Akkermansia	Increased	----	*Akkermansia muciniphila*, used as a probiotic, improved metabolic health in obese patients[100] Increased in Parkinson's patients[93] Increased in children with Autism[98]
Butyricimonas	Decreased	Butyrate (T_{REG} cells and M2 inducer) producing microbe in mice[16,90,91].	Increased in Vitamin D cell receptor knock out mice[87]
Collinsella	Decreased	----	Increased on colorectal cancer tissues[101] Increased in symptomatic atherosclerosis patients[102]
Slackia	Decreased	*Slackia equolifaciens sp. nov.* can produce antioxidants that can induce apoptosis in tumor cells[101,103,104]	Increased on colorectal cancer tissues[101]
Prevotella	Decreased	----	Decreased in Parkinson's patients[94] Increased in Vitamin D cell receptor knock out mice[87] Reduced in autistic children[105] *Prevotella copri* increases susceptibility to arthritis[106]
Faecalibacterium	Decreased (vitamin D insufficient)[80]	Butyrate (T_{REG} cells and M2 inducer) producing microbe in mice[16,90,91].	Decreased in Parkinson's patients[94] Decreased in children with Autism[98] Decreased *Faecalibacterium prausnitzii* in Crohn's disease and ulcerative colitis patients[95,107] Increased in allergic asthma patients[108]
Desulfovibrionaceae	Increased (pediatric)	----	Increased abundance in mice with impaired glucose intolerance[109]
Lachnospiraceae	Decreased (pediatric)	----	Decreased in Parkinson's patients[93] Reduced in patients with colorectal cancer[110]
Ruminococcaceae	Decreased (pediatric)	----	Decreased *Ruminococcus callidus* and increased *Ruminococcus bromii* in Parkinson's patients[94] Increased *Ruminococcus lactaris* in rheumatoid arthritis patients[111] Decreased in children with Autism[98] Decreased *Ruminococcus gnavus* and *Ruminococcus torques* in Crohn's disease patients[95]
Clostridia XIVa and *IV Clusters*[112]	Decreased	Induces colonic T_{REG} cells[113,114]	*Clostridium leptum* decreased in patients with Crohn's disease and ulcerative colitis[107] Clostridium is reduced in patients with food sensitization[97]
Bacteroides[112]	Decreased	*Bacteroides fragilis* increased T_{REG} cells and IL-10 productiton[115]	Decreased *Bacteroides vulgatus* and *Bacteroides caccae* in Crohn's disease patients[95]

Table 1.1 Microbial populations altered in MS patients and their inflammatory implications.

1.5 Probiotics and EAE/MS

Probiotics have demonstrated therapeutic potential in both neuroinflammatory murine and human studies. In murine models, administration of *Lacotobacillus* and *Bifidobacterium* can reduce EAE clinical scores, however the efficacy of probiotic treatment depends on the specific species and strain[10,116,117] (**Table 1.2**). Specifically, probiotic administration of *Lactobacillus plantarum* DSM 15312 and *L. paracasei* DSM 13434 were able to reduce EAE clinical scores and lower the percentage of CD4 T cell infiltration into the CNS. Additionally, *L. paracasei* DSM 13434 increased levels of IL-10 and the T_H2 associated cytokine, IL-4[116]. Moreover, mice induced with EAE and gavaged with the probiotic mixture of the *Lactobacillus* strains *L. paracasei* DSM 13434 and *L. plantarum* DSM 15312/15313 had lower clinical scores that were associated with reduced levels of IL-17 in the CNS and IFNγ in the spleen (ELISA of MOG_{35-55} stimulated spleen supernatant), as well as an increased frequency IL-10^+ T_{REG} cells in the CNS[116]. Furthermore, a probiotic mixture containing *L. casei*, *L. acidophilus*, *L. reuteri*, *B. bifidum*, and *Streptococcus thermophilus* decreased EAE clinical scores and increased IL-10 and IL-4-producing T cells[118]. In contrast, a probiotic mixture used in an EAE guinea pig model, composed of *B. breve* and *L. casei* did not impact disease pathogenesis[117]. The efficacy of probiotic administration was demonstrated in a rat EAE model, which revealed that probiotic administration of *Enterococcus faecium* strain L-3 ameliorated disease to the same extent as the MS drug glatiramer acetate[119,120]. Furthermore, probiotic administration of *Bacteroides fragilis* reduced EAE disease via microbial metabolite polysaccharide A and increased IL-10 production from Foxp3+ T_{REG} cells[115]. Collectively, these murine studies demonstrate that probiotics, depending on the species and strain, are effective at dampening EAE clinical scores.

In one small human trial investigating the efficiency of probiotic administration in MS patients, a combination of *L. acidophilus*, *L. casei*, *B. bifidum* and *L. fermentum* decreased the Expanded Disability Status Scale (a scoring system of disease in MS patients)[121]. Another small MS patient study found that taking a probiotic mixture consisting of *Lactobacillus*, *Bifidobacterium* and *Streptococcu*s (*L. paracasei DSM 24734*, *L. plantarum DSM 24730*, *L. acidophilus DSM 24735*, *L. delbruckei DSM 24734*, *B. longum DSM 24736*, *B. infantis DSM 24737*, *B. breve DSM 24732*, and *S. thermophilus DSM 24731*) for two months decreased the relative abundance of disease-associated genera *Akkermansia* and *Blautia*, and reduced peripheral monocytes[122]. Human trials have yielded promising data, however cohort sizes have been relatively small and have thus made drawing firm conclusions difficult. Studies with larger and geographically distinct cohorts would help determine the benefits of probiotics.

Probiotic treatment	**Clinical Scores**	**Immunological impact**	**Inducing agent**	**Disease host**
EAE animal models				
L. paracasei DSM13434[116]	↓ Decrease in clinical scores	↑ IL-4, IL-10 and TGF-β1 secretion from T cells *in vitro* ↓ Percentage of $CD4^+$ T cells in CNS and IFNγ and TNFα secretion from T cells *in vitro*	MOG_{35-55}	C57/BL6J mice
L. plantarum DSM1512[116]	↓ Decrease in clinical scores	↑ T_{REG} in mesenteric lymph nodes	MOG_{35-55}	C57/BL6J mice
L. plantarum DSM1513[116]	↓ Decrease in clinical scores	↑ IL-27 in blood serum ↓ Percentage of $CD4^+$ T cells in CNS	MOG_{35-55}	C57/BL6J mice
L. paracasei DSM13434 and *L. plantarum* DSM1512 + DSM1513[116]	↓ Decrease in clinical scores	↑ Spleen culture IL-10 secretion *in vitro,* Foxp3 expression in cerebellum and percentage of $Foxp3^+CD4^+$ T cells in MLNs and spleens ↓ Spleen culture IFN-γ, TNF-α and IL17 secretion *in vitro*	MOG_{35-55}	C57/BL6J mice
L. casei, L.acidophilus L reuteni, B. bifidum, S. thermophius[118]	↓ Decrease in disease incidence and clinical scores	↑ IL-4 and IL-10 secretion from T cells *in vitro* ↓ Lymphocyte and T cell infiltration, percentage of $Gr1^+$	MOG_{35-55}	C57/BL6J mice

		and/or $CD11b^+$ monocytes and $CD4^+$ T cells in the spinal cord and IFNγ, TNFα and IL-17 secretion from T cells *in vitro*		
E. coli MG1655[119]	↓ Decrease in incidence	----	MOG_{35-55}	C57/BL6J male mice
E. coli Nissle 1917[119]	↓ Decrease in clinical scores	↑ Number of peripheral MOG-specific T cells and draining LN $Foxp3^+CD4^+$ T cells and IL-10 secretion from T cells *in vitro* ↓ Number of spinal MOG-specific T cells and IFNγ, GM-CSF, IL-17 and TNFα secretion from T cells *in vitro*	MOG_{35-55}	C57/BL6J male mice
Bacteroides fragilis[115]	↓ Decrease	↑ Percentage of Foxp3+ regulatory T cells in cervical LNs and expression of: GATA-3, IL-10, SMAD-3 in the brain ↓ Expression of RORγt and IL-17 in the brain	$PLP_{139-151}$	SJL mice
Enterococus faecium L-3[120]	↓ Decrease	↑ Percentage of: $CD3^+$, $CD3^+CD8a^+$ in blood peripheral MOG-specific T cells ↓ Percentage of $CD3^-CD161a^+$ cells in blood (161a activates leukocyte effector functions) and spinal MOG-specific T cells	Encephalitogenic mixture	Wistar rats
B. breve Yakul*t and L.casei* Shirota[117]	No effect	----	Spinal cord homogenate or MBP	LEW/CrlCrl rats and guinea pig (Slc:Hartley)
Multiple Sclerosis patients				
L. acidophilus, L. casei, B. bifidum, L. fermontum[121]	↓ Decrease in EDSS	↓ C-reactive protein, serum insulin	----	RRMS patients
Lactobacillus, Bifidobacterium, Streptococcus[122]	Not provided	↓ Peripheral monocytes, mean CD80 MFI on classical monocytes, HLA-D MFI on DCs, MS risk HLA-DQA1 allele expression	----	RRMS patients

Table 1.2 Impact of probiotics on the pathogenesis of EAE in murine models and multiple sclerosis.

1.6 Types of dietary fiber and their implications in the pathogenesis of EAE

1.6.1 Types of dietary fiber

Dietary fiber is a carbohydrate polymer that in indigestible by the host, and is rather processed by the host's microbiome. It is often used as a broad term, however there many different types of fiber, split into four main categories: water soluble and highly fermentable fibers, intermediately soluble and fermentable, insoluble and slowly fermentable and insoluble and not readily fermentable[123]. The main water soluble and highly fermentable fibers: inulin, guar gum, pectin and resistant starch are degraded by microbial enzymes to produce short chain fatty acids (SCFAs) such as acetate, propionate and butyrate. These SCFAs are recognized by the G-protein coupled host cell receptors GPR41, GPR43 and GPR109A. GPR41 is expressed on polymorphonuclear and dendritic cells and has affinity for propionate>butyrate>acetate. GPR43 is expressed on polymorphonuclear cells, monocytes and mast cells and responds equally to acetate, butyrate and propionate. Finally, the butyrate receptor GPR109A is expressed on DCs, macrophages and epithelial cells[124,125]. Interactions with these receptors can lead to downstream immunological modulation; for example, SCFAs can increase T_{REG} cells in a GPR43 dependent manor – demonstrating the potential of SCFAs to dampen inflammatory conditions[126].

When present in the diet, fermentable fibers can influence SCFA levels locally in the colon and systemically[127]. In a study where patient fecal samples were isolated and cultured under anaerobic conditions, supplementation with either resistant starch, inulin, pectin or guar gum was sufficient to increase acetate production[128]. However, under the same conditions butyrate production was only increased upon supplementation with guar gum or inulin and propionate production only increased with guar gum supplementation[128]. Thus, in healthy patient microbiome cultures, guar gum was able to have the most diverse impact on SCFA production.

However *in vivo*, several studies have demonstrated that a 30% pectin diet increases propionate[127,129]. This discrepancy could be potentially due to microbial differences or the lack of biofeedback from the host in the *in vitro* study. As for guar gum, *in vivo*, it was able to increase all three SCFAs, reflecting the *in vitro* data[130]. In contrast to the water-soluble fibers, the water-insoluble fiber cellulose is broken down into long chain fatty acids (LCFAs)[131]. The ability of dietary fiber to alter immune modulatory molecules demonstrates its importance in immune health and its potential as a supplementary therapy to dampen inflammatory diseases.

1.6.2 Dietary fiber and EAE

Recently, many studies have explored diet as a prospective source of disease amelioration. An EAE study demonstrated diets consisting of supraphysiologic amounts of pectin, a water soluble and fermentable dietary fiber, reduced disease severity in mice. However, the mechanism of protection was not elucidated[129,131]. Moreover, diets supplemented with cellulose, a water insoluble fiber, protected mice from EAE in a spontaneous murine MS model by shifting the mice's immune system towards T_H2 immunity via LCFAs[131]. As dietary fibers are only digested by the gut microbiome, fiber's capability to influence disease deepens the tie between the microbiome and disease – determining whether protection is due to disease ameliorating SCFAs[162] or another microbial metabolite is a promising field to explore. Differences in the effectiveness of dietary alterations between murine models and human studies demonstrates the importance of translating EAE ameliorative conditions to MS patients to see if the dietary intervention can remain efficacious and improve quality of life.

1.7 Hypothesis

The overarching hypothesis of my thesis is that dietary soluble fiber plays a protective role in the murine MS model (EAE), however the extra-intestinal nature of EAE requires supraphysiologic amounts of fiber.

I aimed to determine the effects of soluble fiber on EAE induced murine cohorts. First, I tested the hypothesis that suboptimal levels of dietary fiber exacerbate EAE pathogenesis. To do this, mice were fed diets containing no fiber (0%), a low-fiber diet that mimics the average Canadian fiber diets (2.5%), or a standard fiber diet (5%) that mimics the fiber concentrations recommended by nutritionists[14]. Then, I tested the hypothesis that supraphysiologic amounts of soluble, fermentable fibers (30% pectin, guar gum, inulin or resistant starch) can limit EAE pathogenesis. In all studies, I monitored clinical scores following EAE induction. At harvest, I analyzed the T_H1, T_H17 and T_{REG} compositions in spleens, brains and spinal cords. Finally, I analyzed fecal samples and colon sections to determine how distinct dietary fibers impact microbiota community composition and gut structure. Collectively, information gained from this research program provided a better understanding of how fiber impacts the immune system in the context of neuroinflammation.

Chapter 2: Methods

2.1 Mouse strains, housing and diets

Mice were housed at the University of Columbia (UBC) in the Center for Disease Modeling (CDM) which is a pathogen and murine norovirus-free facility in nonexperimental mice. C57BL/6 mice (from 6-12 weeks old) were either bred in the facility or ordered from Jackson Laboratories. Female mice and bedding were rotated between cages to maintain a similar basal microbiome. For experiments using male mice, only bedding was exchanged between cages. Mice were kept on a 12 hour day/night cycle. Experimental protocols were approved by the UBC ACC and the Biosafety Committee. Diets of 0% dietary fiber 9GKZ, 2.3% dietary fiber 9GKY (1:1 cellulose and guar gum), 5% dietary fiber (1:1 cellulose/guar gum) 9GQP and 5% fiber (cellulose) 57W5 and 30% dietary fibers of inulin, guar gum, resistant starch and pectin (5BX1, 5BSE, 5BAC and 5BSX, respectively) were ordered from Test Diet. Mice fed 30% guar gum diets received special care – food pellets were wet daily/bi-daily in a petri dish or placed in hydrogel to encourage weight stabilization as if this step was excluded, mice lost significant weight. Diets were isocaloric and contained similar levels of macro- and micronutrients other than fiber to ensure that differences observed during disease were due to the change in dietary fiber. Diet specs can be found in Appendix A. Mice were fed diets two weeks prior to intervention and throughout the remainder of each experiment.

2.2 Experimental autoimmune encephalomyelitis model

2.2.1 EAE induction

Two weeks after dietary intervention, mice received a 100µL rear subcutaneous injection of an emulsion containing 200µg neuro-antigen MOG_{35-55} (specific to C57BL/6 mice)

(GenScript, catalog #: RP10245) resuspended in 1mL PBS and 400µg of non-viable *M. tuberculosis H37 Ra* (BD Difco™ Adjuvants) resuspended in 1.1mL of incomplete Freud's adjuvant (IFA) (BD Biosciences, catalog #: DF0639606), making complete Freud's adjuvant (CFA). Mice were also given a 200µL intraperitoneal injection of 200ng of pertussis toxin resuspended in PBS on the day of induction and a second injection of the same reagents, 48 hours later[132].

2.2.2 Murine scoring

Mice were scored on a 5 point scale[132] with 0 = no paralysis, 0.5 = partial tail tonicity lost, 1 = complete tail tonicity lost, 2 = loss in coordinated movement/hind limb paresis, 2.5 = one hind limb paralyzed. 3 = both hind limbs paralyzed, 3.5 = weakness in forearms, 4 = forelimbs paralyzed and 5 = moribund. Mice in high fiber diet experiments were scored for stool consistency: 0 = normal fecal pellet, 1 = no fecal pellet/softer than normal stool, 2 = soft stool and 3 = diarrhea.

Cumulative scores were calculated by adding the daily scores for each individual mouse from onset of disease to endpoint.

2.2.3 Murine monitoring

Mice were weighed and scored for EAE every 24-72 hours after being placed on the diet up until day 6 post EAE induction, then mice were monitored daily. Once mice reached a CHS or EAE score of 2, food pellets and hydrogel were placed on the cage floor.

2.3 Tissue and single cell preparation

Cardiovascular perfusion was performed with at least 15 mL of sterile 4°C PBS (Sigma-Aldrich, catalog #: D8537) immediately after sacrifice. Brains, spinal cords and spleens were extracted for either flow cytometry or histology. For histological analysis, brains and spinal

cords were kept in 10% formaldehyde and paraffin embedded, sectioned at stained by Wax-It (UBC). For flow cytometric analysis, brains and spinal cords were placed in PBS or FACs buffer minus EDTA (buffer recipes can be found in **Table 2.1**) and stored on ice. Brains, spinal cords and spleens were mashed through a 70 μm nylon mesh filters (Falcon, catalog #: CA21008-952) to create single cell suspensions. Spleens were subjected to ACK lysis buffer to remove red blood cells. Brain and spinal cord leukocytes were enriched by Percoll gradient centrifugation. Single cells were suspended in 40% Percoll (Sigma-Aldrich, catalog #: 17-0891-01) (see Table 2.1) and spun with no deceleration for 15 min at 1400 rpm. The SN and fat layer were vacuumed off and the remaining leukocytes washed prior to further analysis.

2.4 Cell stimulation and staining

2-4 million cells from spleens and the entire sample of brains and spinal cords were resuspended in 300μL simulation media (1:1000 BFA (Sigma-Aldrich, catalog #: B6542-5MG), 1:1500 Golgi stop (BD Bioscience, catalog #: 554724), 1:1000 PMA (Sigma-Aldrich, catalog #: P8139) and 1:1000 ionomycin (final concentration of 1ng/mL) (Sigma-Aldrich, catalog #: I0634)) for 3-5 hours at 37°C in a 96 well round bottom plate. After stimulation, cells were washed in PBS and resuspended in 100μL live/dead stain at 1:600 (Thermo Fisher, catalog #: L34957) in PBS for 15 minutes at 4°C in the dark. Cells were washed 1.5 times with PBS and resuspended in the surface stain (1:200-300 antibodies in FACs buffer) for 30 minutes in the dark at 4°C. Cells were washed 1.5 times with FACs buffer and resuspended in Fix/perm solution (Thermo Fisher: eBioscience, catalog #: 00-5521-00) and kept at 4°C for 20-30 minutes. Cells were washed 1.5 times in perm wash buffer (1:10 dilution of perm was concentrate: dH_2O) (BD Biosciences, catalog #: 554723) and resuspended in the intracellular stain (1:100 antibodies in perm wash buffer) for 30 minutes at room temperature (see Table 2.2 for antibodies). Cells

were washed 1.5 times in in perm wash buffer and resuspended in 250 µL of FACs buffer prior to flow cytometric analysis.

2.5 Flow cytometry

Stained samples were run on a BD LSR II equipped with four lasers (BD Bioscience – blue (488nm), yellow/green (561nm), violet (405nm) and red (633nm)). FlowJo (version 10.1r3, Tree Star Inc.) was used during data analysis, in which all dead cells (positive for live/dead stain) were excluded from analysis.

2.6 Histology

2.6.1 Alcian blue and PAS staining

After extraction (colonic slices were taken from the distal colon – cuts were made around the second to last fecal pellet – still intact), tissues were kept in methacarn for 4-24 hours and then sent to Wax-It for paraffin embedding and staining[133]. Horizonal cross-sections 5 µm thick through the fecal pellet were taken in duplicate for each sample, 10 µm apart.

2.6.2 Mucus measurements

Slides obtained from Wax-it were imaged on a ZEISS Axio Observer using ZEN 2.3 software. Mucus widths were measured with the 'line' tool – three measurements were taken per colonic slice (two slices per sample)[134,135], resulting in a total of 6 measurements per mouse. The average of these 6 measurements are presented as a representation of mucus width per mouse.

2.7 RNA extraction and cDNA synthesis

Colon tissues from the proximal colon (the second cm below the cecum) that were stored in RNAlater (Thermo Fisher, catalog #: AM7021) were thawed and added to 600µL of β-mercaptoethanol and TissueLyser II (1:100) (Qiagen, catalog #: 85300) and homogenized with beads at a frequency of 30beats/second for 6 minutes. RNA was extracted using Ambion

PureLink™ RNA Mini Kit, according to the protocol and cDNA synthesized using SuperscriptII reverse transcriptase and random hexamers (Life Technologies, catalog #: N8080127).

2.8 Gene expression measured by qPCR

Gene expression was measured using PowerUp SYBR Green Master Mix and the supplier's protocol was followed (Applied Biosystems) on a Quant Studio 3 Real-Time PCR System. The gene expression of TNF-α (QuantiTech: Mm_Tnf_1_SG) was measured and normalized to *hprt* (QuantiTech: Mm_Hprt_1_SG).

2.9 16S sequencing

All fecal pellets were stored on dry ice and then at -80°C for long-term storage. RNA from fecal pellets was extracted as per protocol from the DNeasy PowerSoil Kit (Qiagen, catalog #: 12888-100). Purity for each sample and negative controls was checked by nanodrop. PCR quantification was performed by Rachel Simister from the Crowe Lab, UBC. Samples were sent for 16S rRNA gene profiling down to the genera level. SOBS (observed richness - # of OTUs) were calculated using the estimated OTUs. Data analysis was done in collaboration with Rachel Simister using the Mothur progam[136].

Buffer	**Components**
Wash buffer	10mL of Neo-natal calf serum (NCS) in DMEM or RPMI
Complete tissue culture media (CTCM)	450 mL of RPMI or DMEM 50 mL of 100% Fetal bovine serum (FBS) 5 mL of 200μM L-Glutamine 5 mL of 5000U/mL Penicillin-streptomycin 12.5 mL of 1M HEPES 500 μL of 55mM β-mercaptoethanol
FACs buffer	500 mL of PBS 20 mL of 100% neonatal calf serum (NCS) 2 mL of 500mM EDTA
ACK lysis buffer	1L dH_2O 8.29 g of NH_4Cl 1 g $KHCO_3$

	0.0367 g of EDTA
40% Percoll	For 150mLs: 6 mL 10x PBS 54 mL Percoll 90 mL serum-free media
MacConkey agar plates	1 L of dH_2O 50g of MacConkey agar 10g of Difco™ Granulated agar
Mathacarn	60% methanol 30% chloroform 10% glacial acetic acid

Table 2.1 Buffers

Antibody	Channel	Supplier/catalog	Concentration
IL-17a APC	APC	eBioscience™, catalog #: 17-7177-81	1/100
Foxp3 (Ax700)	Ax700	eBioscience™, catalog #: 56-5773-82	1/100
CD44	APC-Cy7	Biolegend, catalog #: 103028	1/300
CD3	Pacific Blue	eBioscience™, catalog #: 48-0033-82	1/300
CD19	PE-Cy7	eBioscience™, catalog #: 25-0193-82	1/300
CD8α	PE Texas red	Invitrogen, catalog #: MCD0817	1/300
CD25	PE	eBioscience™, catalog #: 12-0251-82	1/300

IFNγ	PerCP Cy5.5	eBioscience™, catalog #: 45-7311-82	1/100
IL-17a	PE Texas red	Biolegend, catalog #: 506938	1/100
Foxp3	Ax 488	eBioscience™, catalog #: 53-5773-82	1/100
CD45.2	Ax700	Biolegend, catalog #: 109822	1/300
CD3	PerCP Cy5.5	Biolegend, catalog #: 100218	1/300
B220	APC-Cy7	eBioscience™, catalog #: 47-0452-82	1/300
CD8α	e650	BD Horizon™, catalog #: 563234	1/300
CD4	PE-Cy7	eBioscience™, catalog #: 25-0041-82	1/300
IFNγ	PE	Biolegend, catalog #: 505808	1/100
IL-10	APC	Biolegend, catalog #: 505010	1/100
TCR-β	PerCP Cy5.5	Biolegend, catalog #: 109228	1/300
IFNγ	Pacific Blue	eBioscience™, catalog #: 48-7311-82	1/100
CD11c	e650	eBioscience™, catalog #: 64-0114-82	1/300
CD11b	PE Texas red	Biolegend, catalog #: 101256	1/300
CD103	FITC	eBioscience™, catalog #: 11-1031-82	1/300

Ly6G	Pacific Blue	BD Horizon™, catalog #: 560603	1/300
Ly6C	PE-Cy7	BD Pharmingen™ catalog #: 560593	1/300
NK1.1	PE	eBioscience™, catalog #: 12-5941-63	1/300

Table 2.2: Antibodies

Chapter 3: Results

3.1 Zero-fiber diets do not exacerbate disease when compared to standard fiber diets

3.1.1 Zero-free diets displayed no significant differences in disease severity

Canadians have one of the highest rates of MS and on average do not meet the fiber consumption recommendations, however the impact of this nutritional deficit on MS susceptibility remains unclear[137,138]. Furthermore, past literature has demonstrated that zero-fiber diets exacerbated inflammatory conditions[127,135]. Therefore, we sought to test the hypothesis that zero-fiber diets would lead to exacerbated disease in the murine model of MS, EAE. To test this hypothesis, we selected diets mimicking the recommended amounts of fiber for Canadians according to the Government of Canada[138] (5%), the average amount of fiber that Canadians actually consume (2.5%) and zero-fiber diets. To determine whether the type of dietary fiber differentially impacts disease, I used two standard fiber diets that contained either cellulose, a non-readily fermented fiber, or a mixture of cellulose and the highly fermentable fiber guar gum. Mice were fed diets consisting of 5% cellulose (standard), 5% cellulose and guar gum (1:1) (standard C+G) , 2.3% cellulose and guar gum (low-fiber) (1:1) and 0% fiber (zero-fiber) diets two weeks prior to EAE induction and throughout the course of disease. Mice were induced by a subcutaneous injection containing 400µg of *M. tuberculosis* and 200µg MOG_{35-55} peptide. Mice also received an intraperitoneal injection of 200ng of pertussis toxin on day 0 and day 2 to permeabilize the BBB. Disease severity in the context of ascending paralysis was measured for 15-25 days, with clinical scores in our facility starting to appear between days 6-9 post-induction. No significant differences in disease paralysis were observed across standard, standard C+G, low-fiber and zero-fiber diets. Clinical scores and disease incidence were recorded from

five separate experiments (the standard cellulose diet was used in 4 experiments and standard cellulose and guar gum diet was used in 2 with a total n=5, however results were consistent so no additional repeats were performed). Clinical scores and the percentage of mice that developed disease were pooled together and no differences were observed (**Fig 3.1A-B**). Experiments were performed in two facilities to investigate whether the diets would have differential effects in another facility with a more diverse microbiota, however the data remained consistent. These data demonstrate that zero-fiber diets displayed no beneficial or detrimental effects on disease onset, severity or progression when compared to diets mimicking the recommended and actual consumption of dietary fiber in Canadian populations.

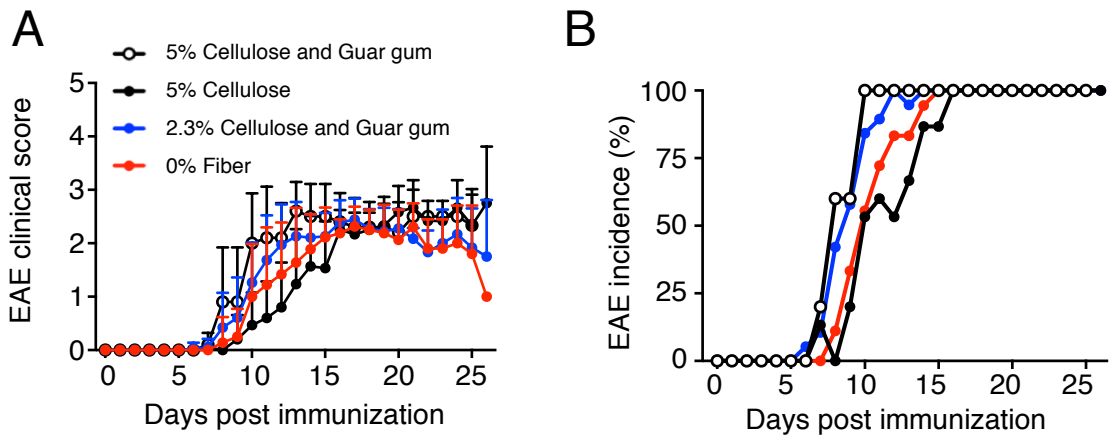

Figure 3.1: Zero-fiber diets did not exacerbate EAE disease. (A) Mice fed diets two weeks prior to induction, and then monitored for levels of paralysis. (B) The fraction of mice that developed disease each day post induction was compiled from five independent experiments.

3.1.2 Immune populations in the CNS and periphery were unaffected by low- or zero-fiber diets

Even though no differences in paralysis was observed, we wanted to address whether the lack of fiber impacted EAE pathogenic immune populations. Mice from 3.1.1 that were fed either standard cellulose, standard cellulose and guar gum, low fiber or zero fiber diets and induced with EAE were sacrificed on day 15-25 post induction and brains, spinal cords and spleens were extracted for tissue processing and staining (some tissues were taken for histology instead of immune cell analysis). Processed tissues were stained with antibodies, run through a flow cytometer and analyzed to determine the cell counts and frequencies of pathogenic IFN- γ (T_H1) and IL-17a (T_H17) producing CD4+ T cells, as well as the protective CD4+ $Foxp3^+$ T_{REG} cells. Across all diets, no differences in CD4+ T cell frequencies or counts were observed in the brain or spinal cord (**Fig 3.2A-C**). In addition to quantifying the total numbers of pathogenic and protective cells in the tissues, we wanted to investigate cellular differentiation and function, using transcription factor expression and cytokine production, to determine if the individual cells from zero-fiber diet fed mice had a more pathogenic phenotype. To do so, an analysis of expression level per cell was performed. However, the mean fluorescence intensity (MFI) of Foxp3, IFNγ, IL-17a in T_{REG}, T_H1 and T_H17 cell subsets were consistent between standard, low and zero-fiber diet treated mice (**Fig 3.2C**). These data are consistent with the lack of differences in clinical scores between diets, demonstrating that a lack of dietary fiber does not significantly influence disease scores or the priming or function of immune cells involved in EAE pathogenesis.

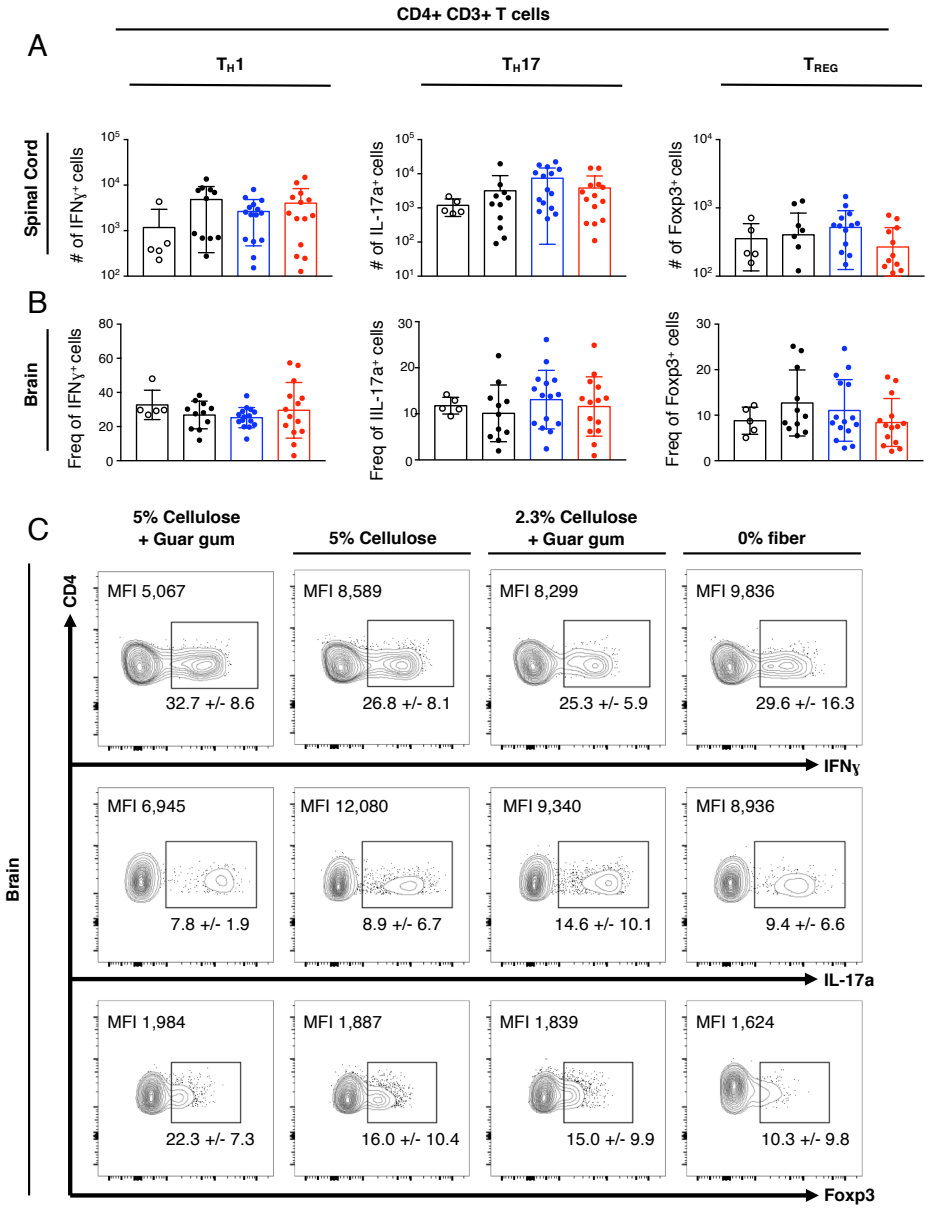

Figure 3.2: Standard-fiber diets did alter EAE associated T cells. (A-C) T cell profiles from EAE mice were analyzed in spinal cord and brain tissues through Ab staining and flow cytometry. The following antibodies were used: CD3 to isolate T cells, CD4 to select T helper cells and either IFNγ, IL-17a or Foxp3 to identify the T cell as a T_H1, T_H17, or T_{REG} cell, respectively. Statistics were calculated using one-way ANOVA.

3.1.3 Microbiome differences between standard- and zero-fiber diet fed mice

As dietary fiber modulates the microbiome[135], we hypothesized our diets containing varying amounts and types of fiber would significantly alter the microbial populations in the gut. We took fecal samples from mice before and after dietary intervention, along with samples after disease progression to determine whether dietary fiber altered the gut microbiome in naïve and EAE conditions. 16S rRNA gene profiling was performed to profile the microbial community down to the genera level. Samples from naïve and EAE mice fed the four diets were plotted on an ordination (NMDS) plot that used rank orders to visualize community differences in reduced dimensions. No obvious differences were seen across diets on the NMDS plot (**Fig 3.3A**), however when pulling out the standard C+G and zero-fiber diet fed mice, it became apparent that these two diets clustered away from each other (**Fig 3.3B**). This suggests that there was a difference in their core microbiomes. In the absence of fiber, mucus becomes the main food source for microbes (thinning the mucus layer) and consequently microbes that can utilize mucus as a food source gain a competitive advantage in the gut and thus increase in frequency[135]. As expected, in naïve mice the relative abundance of *Akkermansia* – a genus containing a mucus consuming species – increased when fed a zero-fiber diet (**Fig 3.3C-D**). This was consistent with a thinner mucus layer in mice fed a zero-fiber diet compared to controls receiving a standard-fiber diet (**Fig 3.3E**). Collectively, these results indicate that our zero-fiber diets impacted the gut microbiome in naïve conditions yet failed to alter the clinical or immunological outcomes following EAE induction.

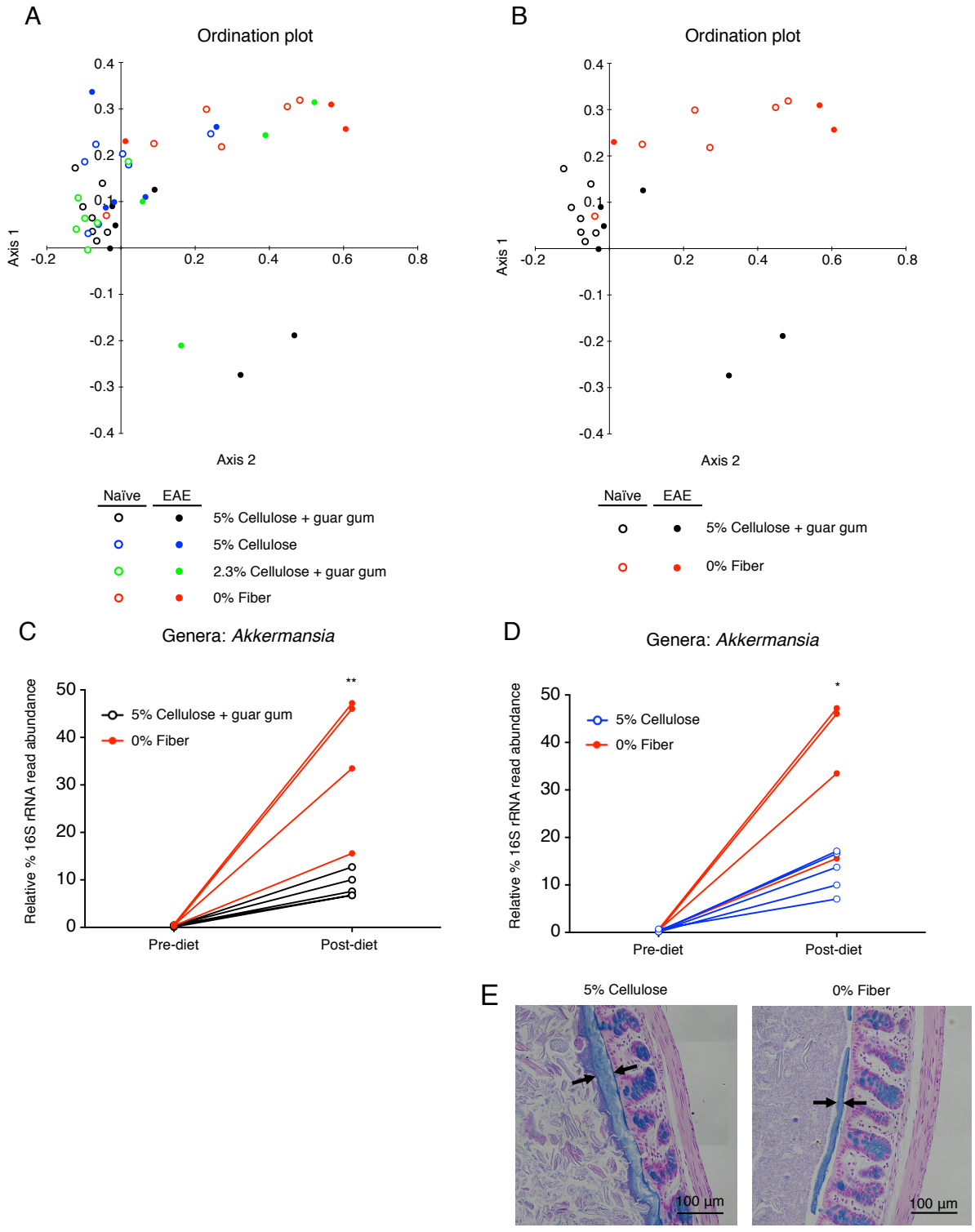

Figure 3.3: Zero-fiber diet impacts intestinal microbiota and mucus. (A-B) The non-metric multidimensional scaling (NMDS) axis were used to plot the location of each naïve and EAE induced mouse sample. The lowest stress for the NMDS axis is 0.0754833 and R^2 for

configuration is 0.97. (C-D) The relative percent of 16S rRNA read abundance of the genera *Akkermansia* for each naïve mouse placed on standard, standard C+G or zero-fiber diets were plotted before and after two weeks of dietary intervention. (E) Colonic slices from the second to last fecal pellet were taken from naïve mice post dietary intervention. Sections were stained with alcian blue dye and then imaged and analyzed using Zen 2.3 software. Statistics were calculated using t tests on prism. For *, $p<0.05$; **, $p<0.005$.

3.2 Guar gum offers ameliorative properties against EAE disease development

While there was no protective effect of a standard amount of dietary fiber, we then considered if due to the peripheral nature of EAE, more drastic diets were required to cause change in disease progression. To address the hypothesis that supraphysiologic amounts of dietary soluble fiber can impact the pathogenesis of EAE, diets were designed containing 30% of four soluble fibers: inulin, guar gum, resistant starch and pectin. This supraphysiologic amount of fiber would be hard to achieve through dietary sources, yet is a common dose in murine studies evaluating the role of fermentable fibers in host physiology[127,129]. These studies have demonstrated that a diet rich in pectin decreased allergic airway disease through a reduction of IL-17 and IL-4 transcription in the lungs, while the same diet exacerbated disease in a serum induced arthritis model. Furthermore, the high pectin diet increased propionate and acetate production and increased *Bacteroidaceae* abundance in the gut. A recent paper observed that mice fed this high pectin diet were protected from EAE, however the mechanism of action was not elucidated and only one fiber type was investigated[129]. My project aimed to test the hypothesis that supraphysiologic doses of single sources of fermentable fibers could

differentially impact EAE disease outcome and immune cell development and function, as well as the microbiota composition.

3.2.1 Clinical Scores and EAE incidence decreased in guar gum fed mice

When mice were fed the soluble fiber diets (30% inulin, guar gum, resistant starch and pectin), the standard cellulose and zero-fiber diets containing similar vitamin, protein and fat proportions, only mice fed 30% guar gum were significantly and reproducibly protected from disease when compared to the standard and zero-fiber diets (**Fig 3.4A-E**). In mice receiving either a standard diet or zero-fiber diets, clinical signs of paralysis developed 7-9 days post-induction (**Fig 3.4A**). In contrast, disease onset was delayed until days 13-15 post-induction in mice receiving the 30% guar gum diet (**Fig 3.4A**). Moreover, the percentage of guar gum-fed mice that developed disease was reduced by nearly 3-fold compared to mice on a standard or zero-fiber diet (**Fig 3.4C**). At the day of sacrifice (day 15 post-induction), mice fed guar gum had a decreased score distribution and lower cumulative disease score (**Fig 3.4D-E**). This data supports the hypothesis that supraphysiologic amounts of dietary fiber can protect mice from EAE and that there are differential effects based on the fiber type. Notably, the 30% pectin diet did not offer any protection from EAE onset or severity. This is in contrast to published data. The reason for these differences is unclear, but may be due to facility-dependent microbiota effects[129]. These data provoke the hypothesis that guar gum may influence EAE pathogenesis directly through immunomodulation or via changes to the microbiota.

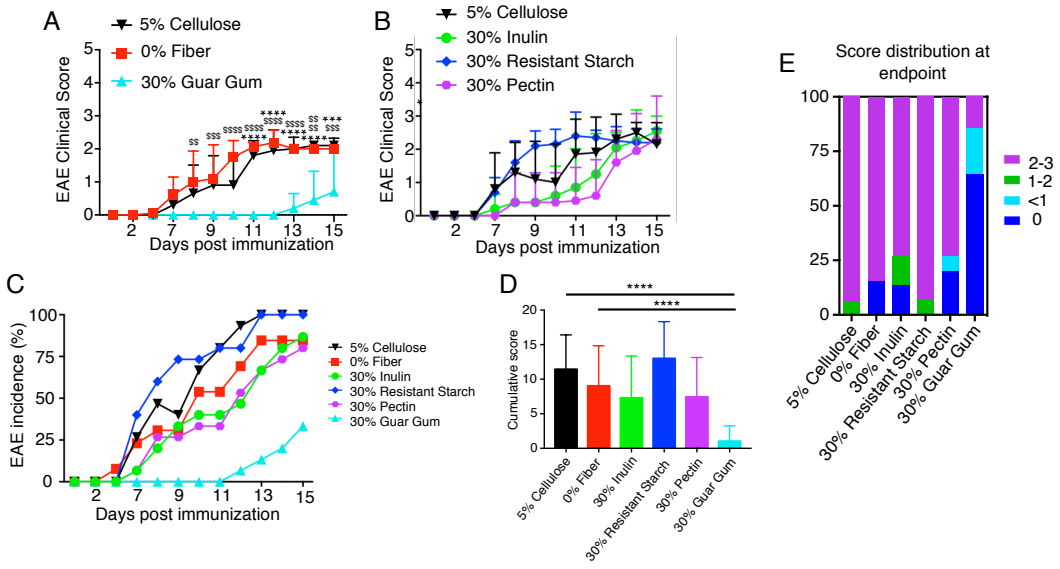

Figure 3.4: Supraphysiologic doses of guar gum offers protection against EAE. (A-B) Mice fed diets two weeks prior to induction, and then monitored for levels of paralysis. Stats were analyzed by two-way ANOVA. */$, p< 0.05; **/$$, p<0.005; ***/$$$, p<0.001. * represents comparison between 30% Guar gum and standard cellulose diets. $ represents comparison between 30% Guar gum and zero-fiber diets. Representative of three independent experiments. (C) The fraction of mice that developed disease within each dietary group was compiled from three independent experiments over the course of 15 days. (D) Cumulative scores of mice from each dietary group across three independent experiments were calculated. Statistics were calculated by t-test. ****, p<0.0001.

3.2.2 Lymphocytic infiltration into the CNS was inhibited in guar gum fed mice

Brains, spinal cords and spleens were taken to analyze EAE pathogenic and protective T cell profiles. The total number of pathogenic IFNγ-producing T_H1 and IL-17a-producing T_H17 cells that infiltrated into the brain was significantly reduced in the guar gum fed mice as

compared to mice fed standard and zero-fiber diets (**Fig 3.5A**). These data could have suggested that the mechanism of disease reduction was due to diminished CNS recruitment of pathogenic cells, however the number of protective $Foxp3^+$ T_{REG} cells found in the CNS was also decreased, indicating a general inhibition of lymphocytic infiltration into the CNS. The number of T_H1 cells in the spinal cord was decreased in guar gum fed mice, however there were no significant differences in T_H17 cell or T_{REG} cells despite a trend in T_{REG} cell reduction (**Fig 3.5A)**. Interestingly, of the few T cells that did enter the CNS of guar gum fed mice, there was no impairment of T_H1 or T_H17 differentiation, indicated by a similar frequency of IFNγ- or IL-17a-producing CD4+ T cells compared to standard diet fed mice (**Fig 3.5B-C**). However, there was a reduction in the frequency of protective T_{REG} cells in the brains of guar gum fed mice (not seen in the spinal cords) (**Fig 3.5B,C**). This reduction could be explained by the reduced number of infiltrating T cells in this group, likely leading to a reduced amount of local inflammatory cytokine production, thereby limiting the need for immune regulation by T_{REG} cells.

While the T cell CNS infiltration was altered in guar gum fed mice, some of those mice didn't develop disease and would therefore bring down the average immune infiltration. It begs the question of whether the immune response in guar gum mice that developed disease was similar or altered compared to standard-diet fed mice that developed disease. To test if guar gum altered immune inflammation once EAE developed, mice that had an EAE score of zero were removed from the analysis. Of the mice that developed disease, there was a non-significant trend in guar gum fed mice to have lower numbers of T_H1 and T_{REG} cells in the brain (**Fig 3.5D**). This suggests that the guar gum fed mice that develop disease have decreased clinical pathogenic immune presentation compared to the control diet fed mice. However, due to the low number of guar gum-fed mice that developed disease and could be included in this analysis, these results

should be interpreted with caution. Notably, one sample from a guar gum mouse that developed disease had much higher T cell infiltration than other mice in the same group, but this mouse did not exhibit the highest clinical score. More experiments would be necessary to determine whether that mouse was an outlier, or if more guar gum diet fed mice that developed disease would demonstrate similar levels of T cell infiltration.

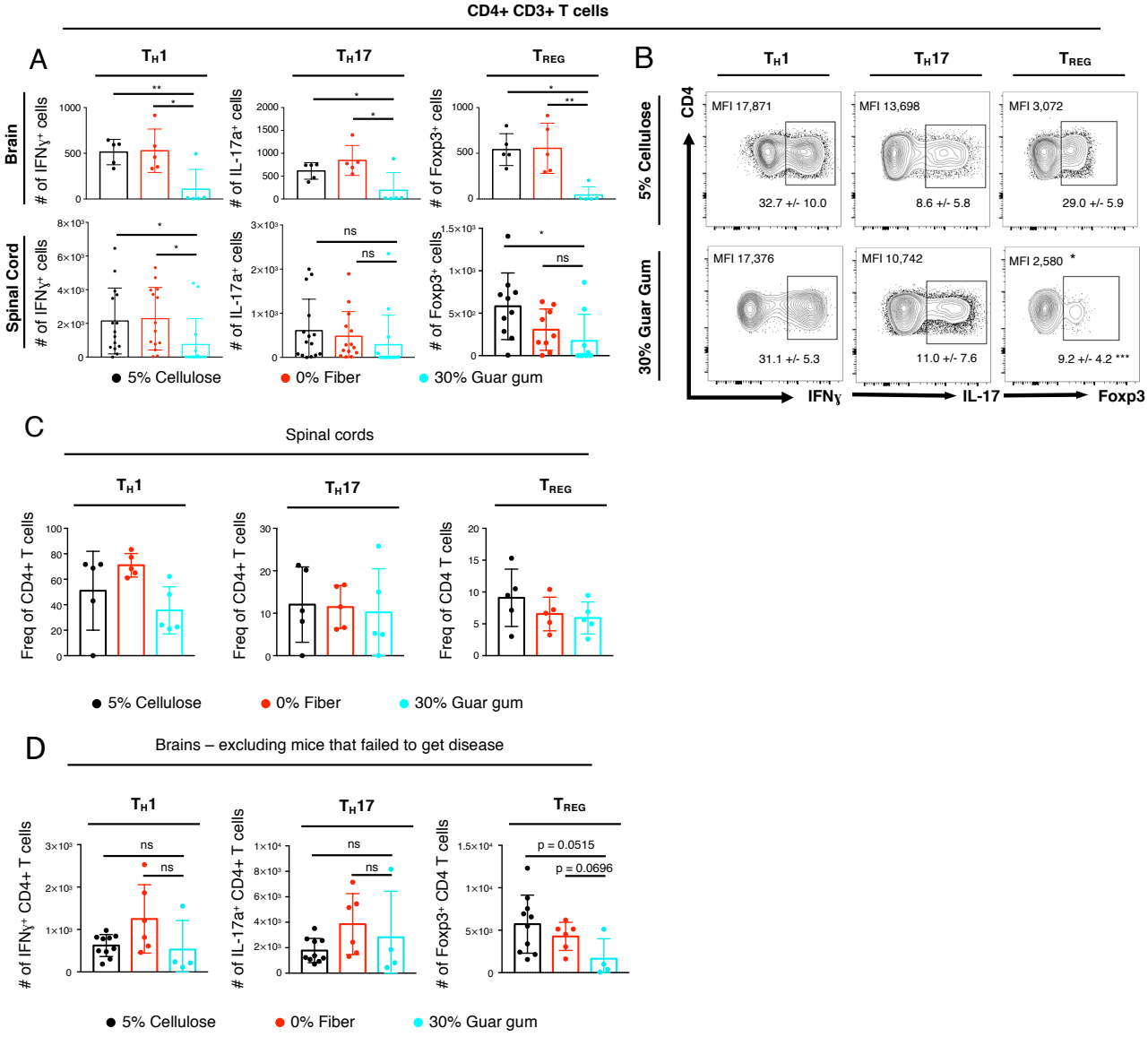

Figure 3.5: Supraphysiologic doses of guar gum prevents T cell CNS infiltration. (A-B) T cell profiles from EAE mice were analyzed in brain and spinal cords through flow cytometry and

antibody staining of CD3 to isolate T cells, CD4 to select T helper cells and either IFNγ, IL-17a or Foxp3 to identify the T cell as a T_H1, T_H17, or T_{REG} cell, respectively. The median cytokine concentration per cell was calculated using MFI in FlowJo. Brains were representative of three independent experiments, 4-5 mice per cohort. Spinal cord populations were compiled from two independent experiments. (C) T cell frequencies from spinal cords were compiled from two independent experiments with similar lymphocytic infiltration. (D) Brain T cell immune profiles from mice that developed disease were compiled from two independent experiments. Statistics were calculated by t-test. For *, $p< 0.05$; **, $p<0.005$; ***, $p<0.001$.

One explanation for the decrease in pathogenic T cells in the brains of guar gum-fed mice could be an impairment of the initial inflammatory immune reaction driven by EAE induction. Alternatively, the autoimmune reaction could occur in the guar gum mice, however something is preventing the pathogenic cells from crossing the blood brain barrier. To test the first hypothesis, I analyzed the differentiation of splenic T_H1, T_H17, and T_{REG} cells at day 15. This analysis revealed no differences in total numbers compared to standard- or zero-fiber diet fed mice (**Fig 3.6A**), suggesting that guar gum, standard- and zero-fiber diet fed mice have similar immune reactions post induction and there is some factor preventing infiltration of autoimmune cells into the CNS in guar gum-fed mice. However, as day 15 is past the peak of EAE peripheral response, it could be too late to detect the early activation stage of EAE in the spleen. Spleens taken at day 9 post EAE induction, thought to be the peak of peripheral EAE activation[139], revealed no differences in T_H1, T_H17, or T_{REG} cell counts (**Fig 3.6B**). This confirmed that the T cell peripheral immune response to EAE induction is the same in the standard diet and 30% guar gum diet fed mice. In addition, the median levels of the adhesion markers VLA-4 and LFA-1

(measured by CD49d and CD11a, respectively) were investigated at day 9 by MFI to determine if guar gum prevented CNS immune infiltration by reducing adherence to the endothelial BBB. However, no significant differences in the levels of these markers on activated (selected by CD44) T helper cells across diets were observed (**Fig 3.6C**). Together, these data suggest that guar gum ameliorates disease progression through inhibition of cellular infiltration into the CNS through an as yet unidentified mechanism.

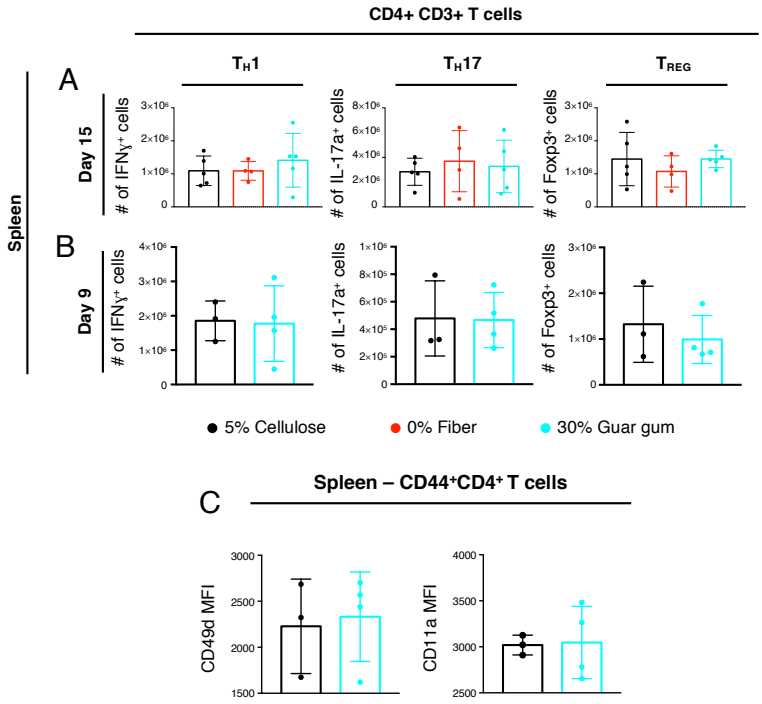

Figure 3.6: Supraphysiologic doses of guar gum does not alter splenic T cell activation or adhesion molecules. (A-B) T cell profiles from EAE mice on either day 15 or 9 were analyzed in spleen tissues through flow cytometry and antibody staining of CD3 to isolate T cells, CD4 to select T helper cells and either IFNγ, IL-17a or Foxp3 to identify the T cell as a T_H1, T_H17, or T_{REG} cell, respectively. Representative of three independent experiments, 4-5 mice per cohort. (C) Mice fed standard or 30% guar gum diets were sacrificed on day 9 post EAE induction and spleens were taken for adhesion marker analysis. Day 15 is representative of three experiments

and day 9 is representative of one experiment. Statistics were calculated by t-test. For *, $p< 0.05$; **, $p<0.005$; ***, $p<0.001$.

3.2.3 The impact of soluble dietary fibers on the microbiome

Because we used diets with large amounts of fiber that readily provides substrates for the gut microbiome, we investigated how the microbial dynamics were altered from diet to diet in naïve and EAE conditions using 16S rRNA gene profiling. As dietary fiber impacts the gut microbiome, we hypothesized that each diet would differentially impact the microbiome in naïve and EAE conditions, in particular, questioning if there was a microbial difference in guar gum fed mice that could explain its mechanism of protection[127,135]. To test this, we first used an ordination plot to see the general microbial landscape of each diet represented in an easy to read two dimensional fashion. In the ordination plot (using NMDS values), the high fiber diets separate from both the standard and zero-fiber diets in both naïve and EAE conditions (**Fig 3.7A**). Except for the 30% resistant starch diet fed mice, EAE and naïve samples place similarly on the plot. In the 30% soluble fiber mice, most of the microbes were derived from the phylum Bacteroidetes in both naïve and EAE conditions (**Fig 3.7B**). On the other hand, in naïve conditions standard diet fed mice had an increased abundance of Firmicutes (the genera *Tyzerella*) and zero-fiber diet fed mice had an increased abundance of Verrucomicrobia (the genera *Akkermansia*) (**Fig 3.7B, D-F**), confirming the results found in **Fig 3.3 C**. Furthermore, when we looked into the microbial community richness using the SOBS index, mice fed a standard fiber diet had the greatest diversity, indicating that a narrower variety of microbes exist efficiently in the absence of fiber or in the presence of a supraphysiologic amount of a select dietary fiber. Alternatively, those extreme conditions may provide a competitive advantage for

select subsets of microbes. Consistent with these observations, in another study that investigated the effect of exposure to a high concentration (26%) of cellulose, a non-fermentable dietary fiber, the microbiome was composed of a reduced number of OTUs[131], suggesting that a wide variety of fibers (both fermentable and non-fermentable) in supraphysiologic amounts limit the variety of microbes that can coexist in the gut. This decrease in diversity in the high fiber diets can partially be explained by increase in the phylum Bacteroidetes. In standard fiber-diet fed mice, Bacteroidetes comprised an average of 45% of the 16S read abundance, but this increased to an average of 82% in each of the high fiber diet fed mice. Within Bacteroidetes, differences between the high fiber diets can be detected at the genera level. In naïve conditions, mice fed 30% guar gum, resistant starch or pectin had increased representation of *Bacteroides*, whereas inulin fed mice had high representation of *Muribaculaceae* (**Fig 3.7D**). However, upon EAE induction, inulin fed mice shift to a *Bacteroides* majority. With these results, no obvious differences in guar gum fed mice's microbiome was observed, suggesting that either guar gum does not protect against EAE in a microbiome dependent manner or that taxonomy needs to be resolved to a species or strain level to reveal differences in community composition.

Microbiomes of MS patients have been reported to have increased proportional abundance of *Akkermansia*, however the question of whether this dysbiosis existed before disease development and contributed to their susceptibility or resulted from disease remains unknown. Investigating microbiome structures in our EAE model before and after disease could provide answers to this question. After EAE induction, the diversity of the standard diet fed mice was decreased (**Fig 3.6C**), most likely due to the decrease in Firmicute abundance and increase in Verrucomicrobia abundance. On the genera level, *Akkermansia* was increased upon EAE induction in standard diet fed mice, which aligns with clinical studies that have observed an

increase in abundance of *Akkermansia* in MS patients[11]. As *Akkermansia* abundance was increased in zero-fiber diet fed mice compared to standard fiber diet fed mice, yet disease did not differ between the two, it suggests that the increase in *Akkermansia* abundance is a result of and not a contributor to disease. Yet, in the 30% fiber diets, *Akkermansia* was not increased after EAE induction – potentially because the amount of fiber overpowers the microbial changes from EAE or the standard diet best mimics the dietary conditions in the MS patients studies, however dietary data was not reported. Altogether, our standard fiber diets were altered after EAE induction to better resemble the microbiomes of MS patients through an increase of *Akkermansia*, suggesting that this change was a result of disease, rather than a causative agent. Further, the development of disease in some of the high-fiber diets without an associated increase in *Akkermansia* suggests that this is not a requirement for nor broadly applicable biomarker of autoimmune neuroinflammation.

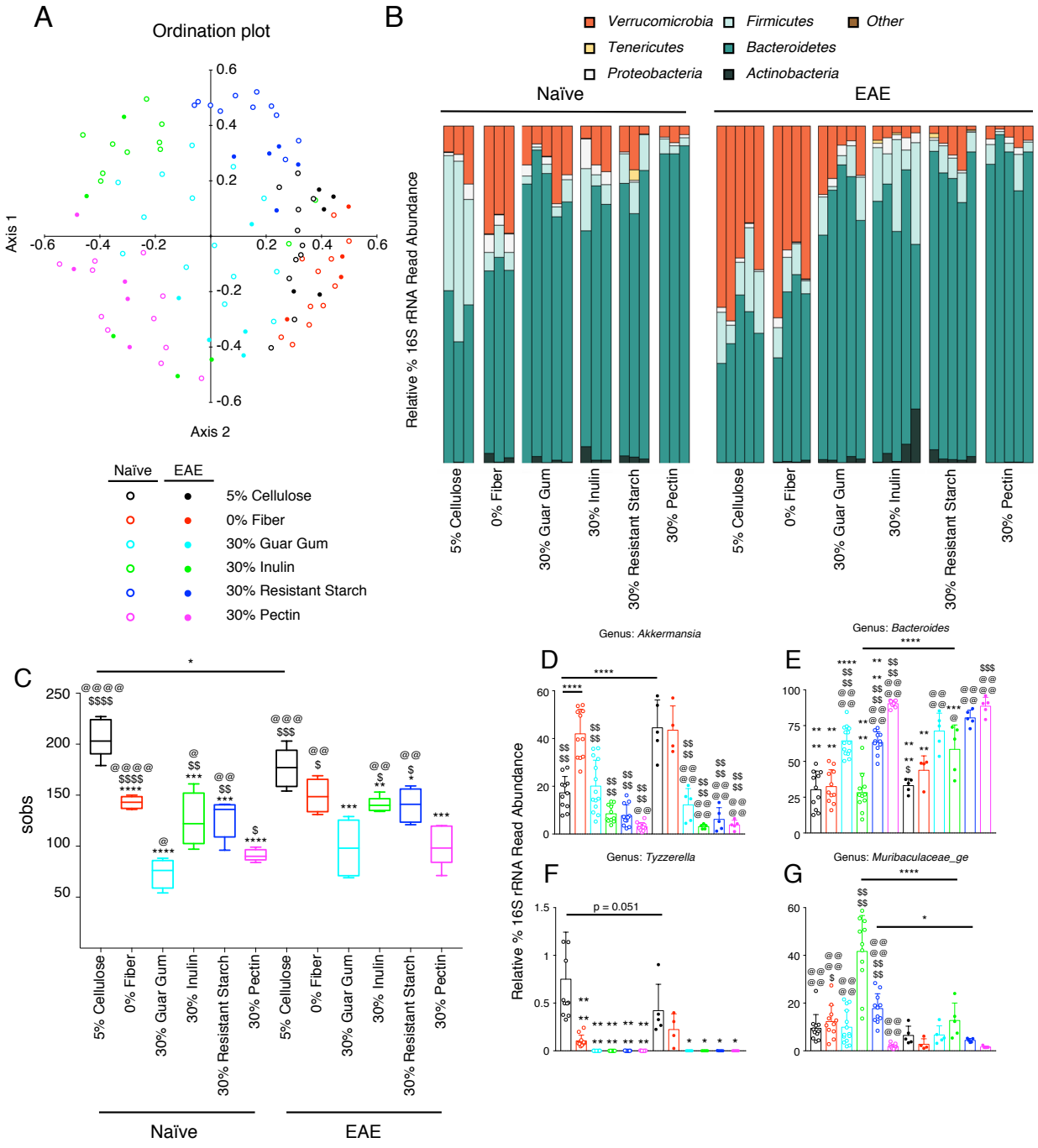

Figure 3.7: Supraphysiologic amounts of soluble fibers cause a shift in the gut microbiome. 16S rRNA gene profiling was performed to analyze microbiome composition down to the genera level. (A) Naïve (from control mice and experimental mice before induction) and EAE (experimental mice post induction) samples were pooled together in an ordinance plot using

NMDS with a lowest stress level of 0.10 and R^2 for configuration of 0.94. (B) Relative percent of 16S rRNA read abundance at the phylum level was calculated. (C) The richness of the microbiomes of mice before and after EAE induction were plotted in a box plot. Statistics were calculated using t-tests where one symbol represents $p< 0.05$, two symbols represent $p<0.005$, three symbols represent $p<0.001$ and four symbols represent $p<0.0001$. */$/@ represent comparisons across diets restricted to either naïve or EAE conditions and a * with a line denotes a change amongst the same diet post EAE induction for (C-G). * represents comparison against the standard diet, $ represents comparison against the 30% guar gum diet and @ represents comparison against the 30% pectin diet. (D-G) Plots represent the relative abundance of microbes at the genera level, where statistics were calculated using one-way ANOVA. (D) $ represents comparison against the 0% fiber diet and @ represents comparison against the standard diet (E) @ represents comparison against the standard diet, $ represents comparison against the 30% inulin diet and * represents comparison against the 30% pectin diet. (F) * represents comparison against the standard diet. (G) @ represents comparison against the 30% inulin diet and $ represents comparison against the 30% pectin diet. Representative of one experiment, with n = 4-5.

3.3 The impact of dietary soluble fibers on the gut

When intestinal barrier integrity is altered, it can leave the host more susceptible to gastrointestinal pathogens[135]. One agent that is essential for the maintenance of the mucus layer is dietary fiber – in the absence of fiber, the mucus thins from degradation by the microbiome[135]. We therefore hypothesized that in the presence of supraphysiologic doses of soluble fibers, the mucus layer would become wider and in the absence of fiber, the mucus layer would become

thinner. To test this, mucus layers stained by alcian blue were measured using ZEN software. However to our surprise, it was observed that the mucus layers of the colons from standard diet fed mice was thicker than those in the mice that were fed 30% diets (inulin displayed a trend in decreased thickness) (**Fig 3.8A-B**). This suggested that perhaps a standard amount of cellulose is a better nutrient source for a wide variety of microbes, supported by the diversity plot in **Fig 3.7C**, which allows microbes to restrict their utilization of the mucus layer as their major nutrient source. Furthermore, perhaps in the select high fiber diet fed mice, the gut microbes that are not able to readily digest that fiber turn to the mucus layer as a food source, resulting in thinner mucus layers. One study found that a high fiber diet rich in a variety of different fiber types led to an increased mucus layer thickness[135]. This, combined with my findings provides evidence that large amounts of one type of fiber does not provide the nutrients necessary to support a diverse microbiome, however a diet consisting of a wide variety fibers can.

To determine whether the zero, standard or high-fiber diets I had tested had an impact on colonic immune cell infiltration, a veterinary pathologist (Dr. Ian Welch, DVM) performed histologic examination of prepared slides. This analysis revealed no differences in colonic immune cell infiltration across all diets (**Fig 3.8A**). However, gene expression analysis revealed diminished expression of the pro-inflammatory cytokine TNFα in guar gum fed mice compared to standard diet fed mice (**Fig 3.8C**). Interestingly, in both dietary conditions, the relative expression TNF-α decreased in response to EAE induction. However as the mouse with the highest EAE score in the guar gum cohort had the highest relative TNF- α expression, this suggests that this effect is more of a product of the induction process, rather than disease onset.

As these supraphysiologic doses of fiber displayed an impact on the microbiome and gut integrity, we further investigated the impact that guar gum had on intestinal homeostasis via

stool consistency. Mice fed 30% guar gum diets developed diarrhea (**Fig 3.8D**). However, this effect could be due to the mice eating softer food because immersing the guar gum pellets in hydrogel was necessary to encourage the food consumption. To control for this, standard fiber diets were immersed in hydrogel, however only the mice fed standard fiber diets pulled out the pellets, limiting the softness of the standard pellets. In the future, diets could be softened before being fed to mice and therefore would determine if guar gum truly leads to uncomfortable side effects or is merely a result of diet administration.

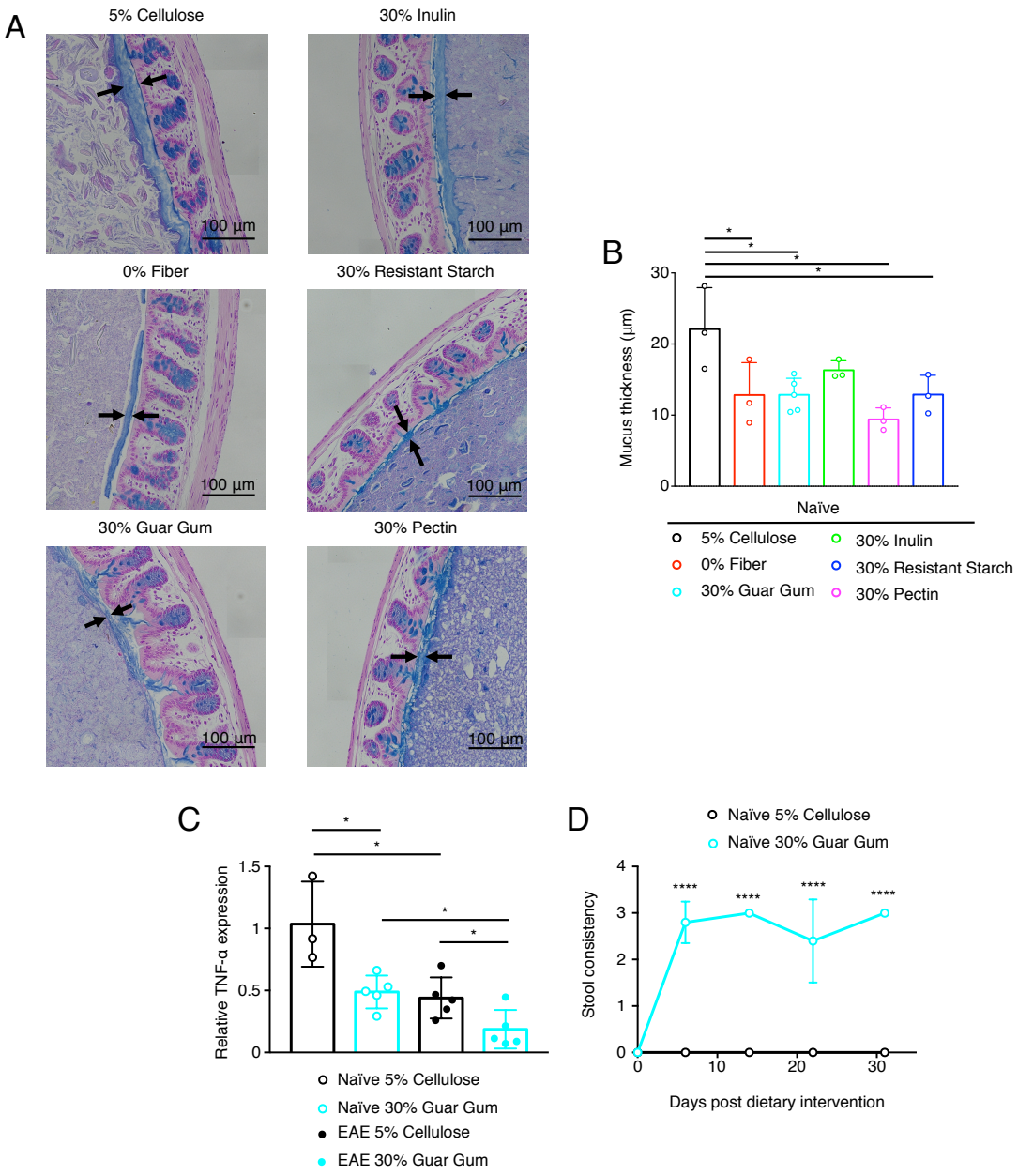

Figure 3.8: The impact of soluble fibers on the gut. (A) Colonic slices from the second to last fecal pellet were taken from naïve mice post dietary intervention. Sections were stained with alcian blue dye and then imaged and analyzed using Zen 2.3 software. The mucus was measure using the line tool for a total of six measurements per mouse and averaged in (B). (C) qPCR for TNF-α was run on proximal colonic samples from naïve and EAE induced mice and was

normalized to the housekeeping gene, hprt. (D) Stool consistency was measured by 0=normal fecal pellet, 1= no fecal pellet or mildly soft fecal pellet, 2=soft fecal pellet or 3=diarrhea.

Chapter 4: Discussion

In this study I aimed to determine how different types of fibers in varying amounts impacted the pathogenesis of EAE and what effects those diets had on the gut at the microbiome and histological level. I discovered that mice fed zero-fiber diets did not have exacerbated EAE disease when compared to mice fed standard fiber diets. Upon this discovery, I decided to investigate how supraphysiologic amounts of soluble fiber impacted the course of disease. I used inulin, guar gum, resistant starch and pectin diets because soluble fibers are digested into SCFAs which, in turn, can have modulatory effects on the host's immune system (increase T_{REG} cells) [127,128,140]. I discovered that one of those soluble fiber diets had a significant impact on the course of disease – guar gum. Guar gum decreased disease severity and the average cumulative score and furthermore, disease onset was significantly delayed. On an immunological level, I discovered that guar gum inhibited T cell infiltration into the brain and T_H1 infiltration into the spinal cord. Peripheral levels of these cells remained the same in the spleens across guar gum and control diets, which suggests that the initial autoimmune reaction occurred in guar gum fed mice, however by some unknown mechanism, lymphocyte infiltration into the CNS was inhibited. In the future, determining if guar gum inhibits disease by dampening the pathogenicity of T cells could be conducted by using the model of passive EAE induction. In this model, encephalogenic T cells are elicited by EAE immunization and then isolated at the peak of the T cell response (day 9) and transferred into new, naïve hosts where the T cells home to the CNS and induce disease. My data has already shown that initial T cell priming is similar between standard and 30% guar gum fed mice, thus immunizing and isolating T cells from these mice would allow one to test the hypothesis that T cells transferred from guar gum-fed mice are impaired in their ability to home to the CNS or bypass the BBB. Furthermore, investigating the

impact of guar gum on other disease associated immune populations in the periphery and CNS, such as DCs and macrophages, could provide more immunological clues as to guar gum's mechanism of protection. Alternatively, guar gum may have an effect on the BBB that limits T cell infiltration of the CNS. The findings that pectin did not offer any significant and reproducible protective effects contradicts a previous study that demonstrated that pectin, at the same level, was able to dampen disease[129]. However this study was conducted at a different facility and as the microbiome plays an integral role in the development of EAE, perhaps microbiome differences led to the varied results[141].

One important thing to note about these diets is that 30% of a diet is an extreme proportion and would be difficult to replicate in human diets as Canadians are recommended to have 5% of their diets consisting of dietary fiber. Other studies that have used these fiber diets have not discussed the limitations of these supraphysiologic fiber diets and their translation to patients. However, there are differences in dietary fiber requirements between mice and people – one study used a murine diet made from a mouse's natural food sources that consisted of approximately 15% dietary fiber[135]. This demonstrates that the diets used in our study were approximately twice as much as the natural murine diet. Taking this into consideration, if these results were translated into patient studies, a 10% fiber diet would be easier to achieve than a 30% fiber diet. Maintaining a 10% guar gum diet would be difficult in human trials, however given the drastic protection against disease, if translated to MS, could be worth it to those patients. As this diet would most likely be used after disease establishment, investigating whether a switch to the guar gum after one disease period in a relapse/remitting murine model would better determine translatability to patient trials. However, given the fact that guar gum inhibits disease by preventing immune translocation into the CNS, rather than inhibiting the

initial peripheral activation response suggests that guar gum might prevent further disease by inhibiting immune cell translocation into the CNS after disease development.

On a microbial level, zero fiber diets displayed a higher abundance of the genera *Akkermansia*, which contains species that can utilize the mucus layer as a nutrient source. Because zero-fiber diets lack a major microbial food source, microbes turn to the mucus layer as a nutrient source and therefore the mucus layer became thinner[135]. At the microbial level, the supraphysiologic soluble fiber diets separated from each other and the standard/zero-fiber diets on an ordination plot. On the phylum level, these high fiber diets had increased Bacteroidetes, suggesting that this phylum best utilizes soluble fibers. Interestingly, my data suggests that the other microbes in the guts of mice fed high fiber diets were not able to rely on the soluble fiber as the nutrient source – mucus layer thickness was decreased in these mice. I hypothesize that the microbes that cannot utilize the soluble fibers as a nutrient source degrade the mucus layer, thereby making it thinner. Having a thinner mucus layer can leave a host more susceptible to gut pathogens, and therefore it is important to take into consideration the side effects of a single high fiber diet[135]. Similar to germ-free mice, which demonstrate that the inability to digest dietary fiber increases cecum size, the cecums from supraphysiologic fiber diet fed mice were increased (data not shown) – supporting the hypothesis that the microbes are not fully utilizing the soluble fibers.

Overall, these data provide important contributions with applications for patient trials that want to utilize diets as a supplementary intervention to modulate disease. As multiple sclerosis does not have a cure and no drug successfully prevents symptoms, an additional therapeutic intervention that could improve the quality of life would be an important field to investigate. Furthermore, my research has targeted the long asked question of whether microbes that are

increased in MS patients are linked to disease pathogenesis or are a reaction to systemic changes caused by disease. *Akkermansia*, previously shown to have species increased in MS patients, was increased in zero-fiber diets compared to standard fiber diets, yet disease pathogenesis between the two cohorts was the same. This demonstrates that an increase in *Akkermansia* does not predispose these mice to more severe disease. Moreover, in standard diet fed mice, *Akkermansia* was increased after EAE induction, aligning with the MS patient study. Although the 30% fiber diet fed mice did not experience this change after EAE induction, this phenomenon could be explained if the pressure caused by the supraphysiologic doses of soluble fibers on microbial communities was greater than the pressure from EAE induction to alter *Akkermansia*, indicating that diet has more of an impact on the gut microbiome than EAE induction. Together, these data suggest that in standard diet conditions, the increase in *Akkermansia* was a reaction to disease, rather than contributing to it. In the future, gavaging mice with *Akkermansia* and other microbes altered in MS patients would determine the roles that they have in the pathogenesis of EAE.

In summary, my thesis provided novel discoveries of the roles of dietary fibers in standard and supraphysiologic levels in the pathogenesis of EAE and the potential of guar gum as a dietary supplemental therapeutic worth investigating in MS patients. In addition, my data provided an analysis of how a wide variety of dietary fibers impact the gut microbiome in naïve conditions, as well as during the pathogenesis of EAE.

References

1. Rahn, K., Slusher, B. & Kaplin, A. Cognitive impairment in multiple sclerosis: a forgotten disability remembered. *Cerebrum* **2012,** 14 (2012).
2. Chiaravalloti, N. D. & Deluca, J. Cognitive impairment in multiple sclerosis - neurologie. *Lancet Neurol.* **7,** 1139–1151 (2008).
3. Van Emmerik, R. E. A., Remelius, J. G., Johnson, M. B., Chung, L. H. & Kent-Braun, J. A. Postural control in women with multiple sclerosis: Effects of task, vision and symptomatic fatigue. *Gait Posture* **32,** 608–614 (2010).
4. Bradl, M. & Lassmann, H. Progressive multiple sclerosis. *Semin. Immunopathol.* **31,** 455–465 (2009).
5. Ontaneda, D. & Fox, R. J. Progressive multiple sclerosis. *Curr. Opin. Neurol.* **28,** 237–243 (2016).
6. Kieseier, B. C. & Hartung, H. P. Current disease-modifying therapies in multiple sclerosis. *Semin. Neurol.* **23,** 133–145 (2003).
7. Swank, R. L. & Dugan, B. B. Effect of low saturated fat diet in early and late cases of multiple sclerosis. *Lancet* **336,** 37–39 (1990).
8. Thacker, E. L., Mirzaei, F. & Ascherio, A. Infectious mononucleosis and risk for multiple sclerosis: A meta-analysis. *Ann. Neurol.* **59,** 499–503 (2006).
9. Kurtzke, J. F., Beebe, G. W. & Norman, J. E. Epidemiology of multiple sclerosis in U.S. veterans. *Neurology* **29,** 1228 LP-1228 (1979).
10. Maassen, C. B. M. & Claassen, E. Strain-dependent effects of probiotic lactobacilli on EAE autoimmunity. *Vaccine* **26,** 2056–2057 (2008).
11. Jangi, S. *et al.* Alterations of the human gut microbiome in multiple sclerosis. *Nat.*

Commun. **7,** (2016).

12. Chen, J. *et al.* Multiple sclerosis patients have a distinct gut microbiota compared to healthy controls. *Sci. Rep.* **6,** 1–10 (2016).
13. Tremlett, H. *et al.* Gut microbiota in early pediatric multiple sclerosis: a case−control study. *Eur. J. Neurol.* **23,** 1308–1321 (2016).
14. Takahashi, K. *et al.* Reduced Abundance of Butyrate-Producing Bacteria Species in the Fecal Microbial Community in Crohn's Disease. *Digestion* **93,** 59–65 (2016).
15. Shaw, K. A. *et al.* Dysbiosis, inflammation, and response to treatment: A longitudinal study of pediatric subjects with newly diagnosed inflammatory bowel disease. *Genome Med.* **8,** 1–13 (2016).
16. Zhang, M. *et al.* Butyrate inhibits interleukin-17 and generates Tregs to ameliorate colorectal colitis in rats. *BMC Gastroenterol.* **16,** 1–9 (2016).
17. Schuh, C. *et al.* Oxidative tissue injury in multiple sclerosis is only partly reflected in experimental disease models. *Acta Neuropathol.* **128,** 247–266 (2014).
18. Arima, Y. *et al.* A pain-mediated neural signal induces relapse in murine autoimmune encephalomyelitis, a multiple sclerosis model. *Elife* **4,** 1–23 (2015).
19. Torkildsen, Brunborg, L. A., Myhr, K. M. & Bø, L. The cuprizone model for demyelination. *Acta Neurol. Scand.* **117,** 72–76 (2008).
20. Viglietta, V., Baecher-Allan, C., Weiner, H. L. & Hafler, D. A. Loss of Functional Suppression by CD4 $^{+}$ CD25 $^{+}$ Regulatory T Cells in Patients with Multiple Sclerosis. *J. Exp. Med.* **199,** 971–979 (2004).
21. Pierson, E. R., Stromnes, I. M. & Goverman, J. M. B cells promote induction of experimental autoimmune encephalomyelitis by facilitating reactivation of T cells in the

CNS. *J. Immunol.* **192,** 929–939 (2014).

22. Liu, C. *et al.* Targeting the Shift from M1 to M2 Macrophages in Experimental Autoimmune Encephalomyelitis Mice Treated with Fasudil. *PLoS One* **8,** (2013).
23. Mohammad, M. G. *et al.* Dendritic cells and multiple sclerosis: Disease, tolerance and therapy. *Int. J. Mol. Sci.* **14,** 547–562 (2013).
24. Reindl, M. *et al.* Antibodies against the myelin oligodendrocyte glycoprotein and the myelin basic protein in multiple sclerosis and other neurological diseases: a comparative study. *Brain* **122,** 2047–56 (1999).
25. von Büdingen, H. C., Harrer, M. D., Kuenzle, S., Meier, M. & Goebels, N. Clonally expanded plasma cells in the cerebrospinal fluid of MS patients produce myelin-specific antibodies. *Eur. J. Immunol.* **38,** 2014–2023 (2008).
26. Storch, M. K. *et al.* Multiple sclerosis: In situ evidence for antibody- and complement-mediated demyelination. *Ann. Neurol.* **43,** 465–471 (1998).
27. Liu, Y. *et al.* Myelin-specific multiple sclerosis antibodies cause complement-dependent oligodendrocyte loss and demyelination. *Acta Neuropathol. Commun.* **5,** 25 (2017).
28. Ulvestad, E. *et al.* Reactive microglia in multiple sclerosis lesions have an increased expression of receptors for the Fc part of IgG. *J. Neurol. Sci.* **121,** 125–131 (1994).
29. Lehmann-Horn, K., Kronsbein, H. C. & Weber, M. S. Targeting B cells in the treatment of multiple sclerosis: recent advances and remaining challenges. *Ther. Adv. Neurol. Disord.* **6,** 161–173 (2013).
30. Rojas, O. L. *et al.* Recirculating Intestinal IgA-Producing Cells Regulate Neuroinflammation via IL-10. *Cell* **176,** 610–624.e18 (2019).
31. Molnarfi, N. *et al.* MHC class II–dependent B cell APC function is required for induction

of CNS autoimmunity independent of myelin-specific antibodies. *J. Exp. Med.* **210,** 2921–2937 (2013).

32. Li, R. *et al.* Cytokine-defined B cell responses as therapeutic targets in multiple sclerosis. *Front. Immunol.* **6,** 1–10 (2016).

33. Barr, T. A. *et al.* B cell depletion therapy ameliorates autoimmune disease through ablation of IL-6–producing B cells. *J. Exp. Med.* **209,** 1001–1010 (2012).

34. Li, R. *et al.* Proinflammatory GM-CSF-producing B cells in multiple sclerosis and B cell depletion therapy. *Sci. Transl. Med.* **7,** 310ra166 (2015).

35. Knippenberg, S. *et al.* Reduction in IL-10 producing B cells (Breg) in multiple sclerosis is accompanied by a reduced naïve/memory Breg ratio during a relapse but not in remission. *J. Neuroimmunol.* **239,** 80–86 (2011).

36. Mï¿½rquez, A. C. & Horwitz, M. S. The role of latently infected B cells in CNS autoimmunity. *Front. Immunol.* **6,** (2015).

37. Shen, P. *et al.* IL-35-producing B cells are critical regulators of immunity during autoimmune and infectious diseases. *Nature* **507,** 366–370 (2014).

38. Ivanov, I. I. *et al.* The Orphan Nuclear Receptor RORγt Directs the Differentiation Program of Proinflammatory IL-17+ T Helper Cells. *Cell* **126,** 1121–1133 (2006).

39. Liblau, R. S., Singer, S. M. & McDevitt, H. O. Th1 and Th2 CD4+ T cells in the pathogenesis of organ-specific autoimmune diseases. *Immunol. Today* **16,** 34–8 (1995).

40. Liu, Y., Teige, I., Birnir, B. & Issazadeh-Navikas, S. Neuron-mediated generation of regulatory T cells from encephalitogenic T cells suppresses EAE. *Nat. Med.* **12,** 518–525 (2006).

41. Bettelli, E. *et al.* Reciprocal developmental pathways for the generation of pathogenic

effector TH17 and regulatory T cells. *Nature* **441,** 235–238 (2006).

42. Jager, A., Dardalhon, V., Sobel, R. A., Bettelli, E. & Kuchroo, V. K. Th1, Th17, and Th9 Effector Cells Induce Experimental Autoimmune Encephalomyelitis with Different Pathological Phenotypes. *J. Immunol.* **183,** 7169–7177 (2009).

43. Serada, S. *et al.* IL-6 blockade inhibits the induction of myelin antigen-specific Th17 cells and Th1 cells in experimental autoimmune encephalomyelitis. *Proc. Natl. Acad. Sci.* **105,** 9041–9046 (2008).

44. Langrish, C. L. *et al.* IL-23 drives a pathogenic T cell population that induces autoimmune inflammation. **201,** 233–240 (2005).

45. Connor, R. A. O. *et al.* Cutting Edge: Th1 Cells Facilitate the Entry of Th17 Cells to the Central Nervous System during Experimental Autoimmune Encephalomyelitis. (2019). doi:10.4049/jimmunol.181.6.3750

46. Durelli, L. *et al.* T-helper 17 cells expand in multiple sclerosis and are inhibited by interferon-β. *Ann. Neurol.* **65,** 499–509 (2009).

47. Voskuhl, R. R. *et al.* T helper 1 (TH1) functional phenotype of human myelin basic protein-specific t lymphocytes. *Autoimmunity* **15,** 137–143 (1993).

48. Olsson, T. *et al.* Autoreactive T lymphocytes in multiple sclerosis determined by antigen-induced secretion of interferon-γ. *J. Clin. Invest.* **86,** 981–985 (1990).

49. Koncarolo, M., Velde, A. te & Figdor, C. Karen Johnson,* Rob Kastelein,* Hans Yssel, and Jan E. de Vries. *Ncbi.Nlm.Nih.Gov* **174,** (1991).

50. Babbe, H. *et al.* Clonal Expansions of Cd8 $^{+}$ T Cells Dominate the T Cell Infiltrate in Active Multiple Sclerosis Lesions as Shown by Micromanipulation and Single Cell Polymerase Chain Reaction. *J. Exp. Med.* **192,** 393–404 (2000).

51. Huseby, E. S. *et al.* A Pathogenic Role for Myelin-Specific Cd8 $^{+}$ T Cells in a Model for Multiple Sclerosis. *J. Exp. Med.* **194,** 669–676 (2001).

52. Hartmann, F. J. *et al.* Multiple sclerosis-associated IL2RA polymorphism controls GM-CSF production in human THcells. *Nat. Commun.* **5,** 1–10 (2014).

53. Rasouli, J. *et al.* Expression of GM-CSF in T Cells Is Increased in Multiple Sclerosis and Suppressed by IFN-β Therapy. *J. Immunol.* **194,** 5085–5093 (2015).

54. Zhang, J. *et al.* A novel subset of helper T cells promotes immune responses by secreting GM-CSF. *Cell Death Differ.* **20,** 1731–1741 (2013).

55. Laar, L. Van De, Coffer, P. J. & Woltman, A. M. Regulation of dendritic cell development by GM-CSF : molecular control and implications for immune homeostasis and therapy. *Development* **119,** 3383–3393 (2012).

56. Huen, S. C. *et al.* GM-CSF Promotes Macrophage Alternative Activation after Renal Ischemia/Reperfusion Injury. *J. Am. Soc. Nephrol.* **26,** 1334–1345 (2015).

57. Ponomarev, E. D. *et al.* GM-CSF Production by Autoreactive T Cells Is Required for the Activation of Microglial Cells and the Onset of Experimental Autoimmune Encephalomyelitis. *J. Immunol.* **178,** 39–48 (2007).

58. Fletcher, J. M. *et al.* CD39+Foxp3+ Regulatory T Cells Suppress Pathogenic Th17 Cells and Are Impaired in Multiple Sclerosis. *J. Immunol.* **183,** 7602–7610 (2009).

59. Furlan, R. *et al.* Activation of invariant NKT cells by αGalCer administration protects mice from MOG35-55-induced EAE: Critical roles for administration route and IFN-γ. *Eur. J. Immunol.* **33,** 1830–1838 (2003).

60. Miyamoto, K., Miyake, S. & Yamamura, T. A synthetic glycolipid prevents autoimmune encephalomyelitis by inducing TH2 bias of natural killer T cells. *Nature* **413,** 531 (2001).

61. Viglietta, V., Baecher-Allan, C., Weiner, H. L. & Hafler, D. A. Loss of Functional Suppression by CD4 $^{+}$ CD25 $^{+}$ Regulatory T Cells in Patients with Multiple Sclerosis. *J. Exp. Med.* **199,** 971–979 (2004).

62. Haas, J. *et al.* Reduced suppressive effect of CD4+CD25high regulatory T cells on the T cell immune response against myelin oligodendrocyte glycoprotein in patients with multiple sclerosis. *Eur. J. Immunol.* **35,** 3343–3352 (2005).

63. Yamasaki, R. *et al.* Differential roles of microglia and monocytes in the inflamed central nervous system. *J. Exp. Med.* **211,** 1533–1549 (2014).

64. Greter, M. *et al.* Dendritic cells permit immune invasion of the CNS in an animal model of multiple sclerosis. *Nat. Med.* **11,** 328–334 (2005).

65. Heink, S. *et al.* Trans-presentation of IL-6 by dendritic cells is required for the priming of pathogenic T H 17 cells. *Nat. Immunol.* **18,** 74–85 (2017).

66. Eugster, H. P., Frei, K., Kopf, M., Lassmann, H. & Fontana, A. IL-6-deficient mice resist myelin oligodendrocyte glycoprotein- induced autoimmune encephalomyelitis. *Eur. J. Immunol.* **28,** 2178–2187 (1998).

67. Wilms, H. *et al.* Dimethylfumarate inhibits microglial and astrocytic inflammation by suppressing the synthesis of nitric oxide, IL-1β, TNF-α and IL-6 in an in-vitro model of brain inflammation. *J. Neuroinflammation* **7,** 1–8 (2010).

68. Imler, T. J. & Petro, T. M. Decreased severity of experimental autoimmune encephalomyelitis during resveratrol administration is associated with increased IL-17+IL-10+T cells, CD4-IFN-γ+cells, and decreased macrophage IL-6 expression. *Int. Immunopharmacol.* **9,** 134–143 (2009).

69. Mikita, J. *et al.* Altered M1/M2 activation patterns of monocytes in severe relapsing

experimental rat model of multiple sclerosis. Amelioration of clinical status by M2 activated monocyte administration. *Mult. Scler. J.* **17,** 2–15 (2011).

70. Voigtl, C. *et al.* Repetitive Injections of Dendritic Cells Matured with Tumor Necrosis Factor ␣ Induce Antigen-speci c Protection of Mice from Autoimmunity. *J. Exp. Med.* **195,** 15–21 (2002).

71. Chieppa, M. *et al.* Cross-Linking of the Mannose Receptor on Monocyte-Derived Dendritic Cells Activates an Anti-Inflammatory Immunosuppressive Program. *J. Immunol.* **171,** 4552–4560 (2003).

72. Miron, V. E. *et al.* M2 microglia and macrophages drive oligodendrocyte differentiation during CNS remyelination. *Nat. Neurosci.* **16,** 1211–1218 (2013).

73. Murray, P. J. & Wynn, T. A. Protective and pathogenic functions of macrophage subsets. *Nat. Rev. Immunol.* **11,** 723–737 (2011).

74. Diehl, J. *et al.* In Vivo Regulation of Experimental Autoimmune Encephalomyelitis by NK Cells: Alteration of Primary Adaptive Responses. *J. Immunol.* **180,** 4495–4506 (2014).

75. Matsumoto, Y. *et al.* Role of natural killer cells and TCRγ δ T cells in acute autoimmune encephalomyelitis. *Eur. J. Immunol.* **28,** 1681–1688 (1998).

76. Stein, M. M. *et al.* Innate Immunity and Asthma Risk in Amish and Hutterite Farm Children. *N. Engl. J. Med.* **375,** 411–421 (2016).

77. Mazmanian, S. K., Round, J. L. & Kasper, D. L. A microbial symbiosis factor prevents intestinal inflammatory disease. *Nature* **453,** 620–625 (2008).

78. Greenblum, S., Turnbaugh, P. J. & Borenstein, E. Metagenomic systems biology of the human gut microbiome reveals topological shifts associated with obesity and in fl

ammatory bowel disease. *Proc. Natl. Acad. Sci.* **109,** 594–599 (2012).

79. Tremlett, H. *et al.* Gut microbiota composition and relapse risk in pediatric MS: A pilot study. *J. Neurol. Sci.* **363,** 153–157 (2016).

80. Cantarel, B. L. *et al.* Gut microbiota in multiple sclerosis: possible influence of immunomodulators. *J. Investig. Med.* **63,** 729–34 (2015).

81. Yatsunenko, T. *et al.* Human gut microbiome viewed across age and geography. *Nature* **486,** 222–227 (2012).

82. David, L. A. *et al.* Diet rapidly and reproducibly alters the human gut microbiome. *Nature* **505,** 559–563 (2014).

83. Kim, E. K. & Choi, E. Biochimica et Biophysica Acta Pathological roles of MAPK signaling pathways in human diseases. *BBA - Mol. Basis Dis.* **1802,** 396–405 (2010).

84. Ochoa-Reparaz, J. *et al.* Role of Gut Commensal Microflora in the Development of Experimental Autoimmune Encephalomyelitis. *J. Immunol.* **183,** 6041–6050 (2009).

85. Berer, K. *et al.* Commensal microbiota and myelin autoantigen cooperate to trigger autoimmune demyelination. *Nature* **479,** 538–541 (2011).

86. Lee, Y. K., Menezes, J. S., Umesaki, Y. & Mazmanian, S. K. Proinflammatory T-cell responses to gut microbiota promote experimental autoimmune encephalomyelitis. *Proc. Natl. Acad. Sci.* **108,** 4615–4622 (2011).

87. Jin, D. *et al.* Lack of Vitamin D Receptor Causes Dysbiosis and Changes the Functions of the Murine Intestinal Microbiome. *Clin. Ther.* **37,** 996–1009.e7 (2015).

88. Kushak, R. *Analysis of the Small Intestinal Microbiome of Children With Autism*. (MASSACHUSETTS GENERAL HOSPITAL BOSTON, 2013).

89. Gao, Z., Guo, B., Gao, R., Zhu, Q. & Qin, H. Microbiota disbiosis is associated with

colorectal cancer. *Front. Microbiol.* **6,** 1–9 (2015).

90. Berni Canani, R. *et al.* Lactobacillus rhamnosus GG-supplemented formula expands butyrate-producing bacterial strains in food allergic infants. *Isme J.* **10,** 742 (2015).

91. Ji, J. *et al.* Microbial metabolite butyrate facilitates M2 macrophage polarization and function. *Sci. Rep.* **6,** 1–10 (2016).

92. Kasai, C. *et al.* Comparison of the gut microbiota composition between obese and non-obese individuals in a Japanese population, as analyzed by terminal restriction fragment length polymorphism and next-generation sequencing. *BMC Gastroenterol.* **15,** 1–10 (2015).

93. Keshavarzian, A. *et al.* Colonic bacterial composition in Parkinson's disease. *Mov. Disord.* **30,** 1351–1360 (2015).

94. Petrov, V. A. *et al.* Analysis of gut microbiota in patients with parkinson's disease. *Bull. Exp. Biol. Med.* **162,** 734–737 (2017).

95. Gevers, D. *et al.* The treatment-naive microbiome in new-onset Crohn's disease. *Cell Host Microbe* **15,** 382–392 (2014).

96. Wu, S. *et al.* Worm Burden-dependent disruption of the porcine colon microbiota by trichuris suis infection. *PLoS One* **7,** (2012).

97. Savage, J. H. *et al.* A prospective microbiome-wide association study of food sensitization and food allergy in early childhood. *Allergy* **73,** 145–152 (2017).

98. De Angelis, M. *et al.* Fecal Microbiota and Metabolome of Children with Autism and Pervasive Developmental Disorder Not Otherwise Specified. *PLoS One* **8,** 1–18 (2013).

99. Clemente, J. C., Ursell, L. K., Parfrey, L. W. & Knight, R. The impact of the gut microbiota on human health: An integrative view. *Cell* **148,** 1258–1270 (2012).

100. Dao, M. C. *et al.* Akkermansia muciniphila and improved metabolic health during a dietary intervention in obesity: Relationship with gut microbiome richness and ecology. *Gut* **65,** 426–436 (2016).

101. Marchesi, J. R. *et al.* Towards the human colorectal cancer microbiome. *PLoS One* **6,** (2011).

102. Karlsson, F. H. *et al.* Symptomatic atherosclerosis is associated with an altered gut metagenome. *Nat. Commun.* **3,** 1245 (2012).

103. Qin, J. *et al.* A human gut microbial gene catalogue established by metagenomic sequencing. *Nature* **464,** 59–65 (2010).

104. Jin, J. S., Kitahara, M., Sakamoto, M., Hattori, M. & Benno, Y. Slackia equolifaciens sp. nov., a human intestinal bacterium capable of producing equol. *Int. J. Syst. Evol. Microbiol.* **60,** 1721–1724 (2010).

105. Kang, D. W. *et al.* Reduced Incidence of Prevotella and Other Fermenters in Intestinal Microflora of Autistic Children. *PLoS One* **8,** (2013).

106. Scher, J. U. *et al.* Expansion of intestinal Prevotella copri correlates with enhanced susceptibility to arthritis. *Elife* **2013,** 1–20 (2013).

107. Kabeerdoss, J., Sankaran, V., Pugazhendhi, S. & Ramakrishna, B. S. Clostridium leptum group bacteria abundance and diversity in the fecal microbiota of patients with inflammatory bowel disease: A case-control study in India. *BMC Gastroenterol.* **13,** (2013).

108. Hevia, A. *et al.* Allergic patients with long-term asthma display low levels of bifidobacterium adolescentis. *PLoS One* **11,** 1–11 (2016).

109. Zhang, C. *et al.* Interactions between gut microbiota , host genetics and diet relevant to

development of metabolic syndromes in mice. *ISME J.* **4,** 232–241 (2009).

110. Ahn, J. *et al.* Human Gut Microbiome and Risk for Colorectal Cancer. *JNCI J. Natl. Cancer Inst.* **105,** 1907–1911 (2013).

111. Zhang, X. *et al.* The oral and gut microbiomes are perturbed in rheumatoid arthritis and partly normalized after treatment. *Nat. Med.* **21,** 895 (2015).

112. Miyake, S. *et al.* Dysbiosis in the gut microbiota of patients with multiple sclerosis, with a striking depletion of species belonging to clostridia XIVa and IV clusters. *PLoS One* **10,** 1–16 (2015).

113. Atarashi, K. *et al.* Induction of Colonic Regulatory T Cells. *Science (80-.).* **331,** 337–342 (2011).

114. Atarashi, K. *et al.* Treginduction by a rationally selected mixture of Clostridia strains from the human microbiota. *Nature* **500,** 232–236 (2013).

115. Ochoa-Reparaz, J. *et al.* Central Nervous System Demyelinating Disease Protection by the Human Commensal Bacteroides fragilis Depends on Polysaccharide A Expression. *J. Immunol.* **185,** 4101–4108 (2010).

116. Lavasani, S. *et al.* A novel probiotic mixture exerts a therapeutic effect on experimental autoimmune encephalomyelitis mediated by IL-10 producing regulatory T cells. *PLoS One* **5,** (2010).

117. Kobayashi, T. *et al.* Oral administration of probiotic bacteria, Lactobacillus casei and Bifidobacterium breve, does not exacerbate neurological symptoms in experimental autoimmune encephalomyelitis. *Immunopharmacol. Immunotoxicol.* **32,** 116–124 (2010).

118. Kwon, H. K. *et al.* Amelioration of experimental autoimmune encephalomyelitis by probiotic mixture is mediated by a shift in T helper cell immune response. *Clin. Immunol.*

146, 217–227 (2013).

119. Secher, T. *et al.* Oral administration of the probiotic strain Escherichia coli Nissle 1917 reduces susceptibility to neuroinflammation and repairs experimental autoimmune encephalomyelitis-induced intestinal barrier dysfunction. *Front. Immunol.* **8,** 1–10 (2017).

120. Abdurasulova, I. N. *et al.* Effects of Probiotic Enterococci and Glatiramer Acetate on the Severity of Experimental Allergic Encephalomyelitis in Rats. *Neurosci. Behav. Physiol.* **47,** 866–876 (2017).

121. Kouchaki, E. *et al.* Clinical and metabolic response to probiotic supplementation in patients with multiple sclerosis: A randomized, double-blind, placebo-controlled trial. *Clin. Nutr.* **36,** 1245–1249 (2017).

122. Tankou, S. K. *et al.* A probiotic modulates the microbiome and immunity in multiple sclerosis. *Ann. Neurol.* **83,** 1147–1161 (2018).

123. Eswaran, S., Muir, J. & Chey, W. D. Fiber and functional gastrointestinal disorders. *Am. J. Gastroenterol.* **108,** 718–727 (2013).

124. Kaji, I., Karaki, S. & Kuwahara, A. Roles of short-chain fatty acids receptors, GPR41 and GPR43 on colonic functions. - PubMed - NCBI. (2017). doi:10.1016/j.annpat.2008.12.001

125. Singh, N. *et al.* Activation of Gpr109a, receptor for niacin and the commensal metabolite butyrate, suppresses colonic inflammation and carcinogenesis. *Immunity* **40,** 128–139 (2014).

126. Colonic, T. *et al.* The Microbial Metabolites, Short-Chain Fatty Acids, Regulate Colonic T Cell Homeostasis. 569–574 (2013).

127. Harris, N. L. *et al.* Gut microbiota metabolism of dietary fiber influences allergic airway disease and hematopoiesis. *Nat. Med.* **20,** 159–166 (2014).

128. Yang, J., Martínez, I., Walter, J., Keshavarzian, A. & Rose, D. J. Invitro characterization of the impact of selected dietary fibers on fecal microbiota composition and short chain fatty acid production. *Anaerobe* **23,** 74–81 (2013).

129. Mizuno, M., Noto, D., Kaga, N., Chiba, A. & Miyake, S. The dual role of short fatty acid chains in the pathogenesis of autoimmune disease models. *PLoS One* **12,** 1–15 (2017).

130. Den Besten, G. *et al.* Protection against the metabolic syndrome by guar gum-derived short-chain fatty acids depends on peroxisome proliferator-activated receptor ? And Glucagon-like peptide-1. *PLoS One* **10,** 1–14 (2015).

131. Berer, K. *et al.* Dietary non-fermentable fiber prevents autoimmune neurological disease by changing gut metabolic and immune status. *Sci. Rep.* **8,** 1–12 (2018).

132. Casiraghi, C. *et al.* Gammaherpesvirus latency accentuates EAE pathogenesis: Relevance to Epstein-Barr virus and multiple sclerosis. *PLoS Pathog.* **8,** 1–16 (2012).

133. Zarepour, M. *et al.* The mucin muc2 limits pathogen burdens and epithelial barrier dysfunction during salmonella enterica serovar typhimurium colitis. *Infect. Immun.* **81,** 3672–3683 (2013).

134. Keeney, K. M. *et al.* Antibiotic Treatment Alters the Colonic Mucus Layer and Predisposes the Host to Exacerbated Citrobacter rodentium -Induced Colitis . *Infect. Immun.* **79,** 1536–1545 (2011).

135. Desai, M. S. *et al.* A Dietary Fiber-Deprived Gut Microbiota Degrades the Colonic Mucus Barrier and Enhances Pathogen Susceptibility. *Cell* **167,** 1339–1353.e21 (2016).

136. Kozich, J. J., Westcott, S. L., Baxter, N. T., Highlander, S. K. & Schloss, P. D. Development of a dual-index sequencing strategy and curation pipeline for analyzing amplicon sequence data on the miseq illumina sequencing platform. *Appl. Environ.*

Microbiol. **79,** 5112–5120 (2013).

137. Warren, S. & Warren, K. G. Prevalence, incidence, and characteristics of multiple sclerosis in Westlock County, Alberta, Canada. *Neurology* **43,** 1760 LP-1760 (1993).

138. Fibre - Canada.ca. Available at: https://www.canada.ca/en/health-canada/services/nutrients/fibre.html. (Accessed: 20th March 2019)

139. Ludwin, S. *et al.* Integration of Th17- and Lymphotoxin-Derived Signals Initiates Meningeal-Resident Stromal Cell Remodeling to Propagate Neuroinflammation. *Immunity* **43,** 1160–1173 (2015).

140. Kato, K. *et al.* Commensal microbe-derived butyrate induces the differentiation of colonic regulatory T cells. *Nature* **504,** 446–450 (2013).

141. Lee, Y. K., Menezes, J. S., Umesaki, Y. & Mazmanian, S. K. Proinflammatory T-cell responses to gut microbiota promote experimental autoimmune encephalomyelitis. *Proc. Natl. Acad. Sci.* **108,** 4615–4622 (2011).

Appendix – Diet specifications

Mod TestDiet® 57W5 w/ No Cellulose, 30% FiberSym 5BAC

DESCRIPTION

Modification of TestDiet® AIN-93G Semi-Purified Diet, 57W5, with no cellulose and 30% FiberSym.

Intended for rodents in a laboratory setting.

CAUTION: Contains a new animal drug for investigational use only in laboratory research animals or for tests in vitro. Not for use in humans.

Storage conditions are particularly critical to TestDiet® products, due to the absence of antioxidants or preservative agents. To provide maximum protection against possible changes during storage, store in a dry, cool location. Storage under refrigeration (2° C) is recommended. Maximum shelf life is six months. (If long term studies are involved, storing the diet at -20° C or colder may prolong shelf life.) Be certain to keep in air tight containers.

*Product Forms Available**	*Catalog #*
1/2" Pellet, Irradiated	1818357-204

**Other Forms Available On Request*

INGREDIENTS (%)

Resistant Wheat Starch	30.0000
Casein - Vitamin Tested	20.0000
Corn Starch	14.7486
Maltodextrin	13.2000
Sucrose	10.0000
Soybean Oil	7.0000
AIN 93G Mineral Mix	3.5000
AIN 93G Vitamin Mix	1.0000
L-Cystine	0.3000
Choline Bitartrate	0.2500
t-Butylhydroquinone	0.0014

**See page 2 for Expanded Ingredient Listings*

FEEDING DIRECTIONS

Feed ad libitum. Plenty of fresh, clean water should be available at all times.

CAUTION:
Perishable - store properly upon receipt.
For laboratory animal use only; NOT for human consumption.

2/3/2018

NUTRITIONAL PROFILE [1]

Protein, %	***18.0***
Arginine, %	0.70
Histidine, %	0.52
Isoleucine, %	0.96
Leucine, %	1.73
Lysine, %	1.45
Methionine, %	0.52
Cystine, %	0.37
Phenylalanine, %	0.96
Tyrosine, %	1.01
Threonine, %	0.77
Tryptophan, %	0.22
Valine, %	1.14
Alanine, %	0.55
Aspartic Acid, %	1.29
Glutamic Acid, %	4.08
Glycine, %	0.39
Proline, %	2.36
Serine, %	1.10
Taurine, %	0.00
Fat, %	***7.2***
Cholesterol, ppm	0
Linoleic Acid, %	3.58
Linolenic Acid, %	0.55
Arachidonic Acid, %	0.00
Omega-3 Fatty Acids, %	0.55
Total Saturated Fatty A	1.10
Total Monounsaturated Fatty Acids, %	1.56
Polyunsaturated Fatty Acids, %	3.85
Fiber (max), %	***22.8***
Carbohydrates, %	***64.6***
Energy (kcal/g) [2]	***3.95***

From:	kcal	%
Protein	0.721	18.2
Fat (ether extract)	0.646	16.4
Carbohydrates	2.584	65.4

Minerals	
Calcium, %	0.54
Phosphorus, %	0.42
Potassium, %	0.36
Magnesium, %	0.05
Sodium, %	0.15
Chloride, %	0.21
Fluorine, ppm	1.0
Iron, ppm	38
Zinc, ppm	35
Manganese, ppm	11
Copper, ppm	6.0
Cobalt, ppm	0.0
Iodine, ppm	0.21
Chromium (added), ppm	1.0
Molybdenum, ppm	0.14
Selenium, ppm	0.24
Vitamins	
Vitamin A, IU/g	4.3
Vitamin D-3 (added), IU/g	1.0
Vitamin E, IU/kg	81.6
Vitamin K, ppm	0.75
Thiamin, ppm	4.8
Riboflavin, ppm	6.7
Niacin, ppm	30
Pantothenic Acid, ppm	16
Folic Acid, ppm	2.1
Pyridoxine, ppm	5.8
Biotin, ppm	0.2
Vitamin B-12, mcg/kg	28
Choline Chloride, ppm	1,250
Ascorbic Acid, ppm	3.6

1. Formulation based on calculated values from the latest ingredient analysis information. Since nutrient composition of natural ingredients varies and some nutrient loss will occur due to manufacturing processes, analysis will differ accordingly. Nutrients expressed as percent of ration on an As-Fed basis except where otherwise indicated.
2. Energy (kcal/gm) - Sum of decimal fractions of protein, fat and carbohydrate x 4,9,4 kcal/gm respectively.

NOTE: When assayed, actual levels may vary from calculated values.

FSSC 22000 www.sgs.com/foodsafety SGS

TestDiet www.testdiet.com

Mod TestDiet® 57W5 w/ No Cellulose, 30% Guar Gum 5BSE

DESCRIPTION

Modification of TestDiet® AIN-93G Semi-Purified Diet, 57W5, with no cellulose and 30% guar gum.

Intended for rodents in a laboratory setting.

CAUTION: Contains a new animal drug for investigational use only in laboratory research animals or for tests in vitro. Not for use in humans.

Storage conditions are particularly critical to TestDiet® products, due to the absence of antioxidants or preservative agents. To provide maximum protection against possible changes during storage, store in a dry, cool location. Storage under refrigeration (2° C) is recommended. Maximum shelf life is six months. (If long term studies are involved, storing the diet at -20° C or colder may prolong shelf life.) Be certain to keep in air tight containers.

*Product Forms Available**	*Catalog #*
1/2" Pellet, Iirradiated	1818358-203

**Other Forms Available On Request*

INGREDIENTS (%)

Guar Gum	30.0000
Casein - Vitamin Tested	20.0000
Corn Starch	14.7486
Maltodextrin	13.2000
Sucrose	10.0000
Soybean Oil	7.0000
AIN 93G Mineral Mix	3.5000
AIN 93G Vitamin Mix	1.0000
L-Cystine	0.3000
Choline Bitartrate	0.2500
t-Butylhydroquinone	0.0014

**See page 2 for Expanded Ingredient Listings*

FEEDING DIRECTIONS

Feed ad libitum. Plenty of fresh, clean water should be available at all times.

CAUTION:
Perishable - store properly upon receipt.
For laboratory animal use only; NOT for human consumption.

2/3/2018

NUTRITIONAL PROFILE [1]

Protein, %	***18.0***
Arginine, %	0.70
Histidine, %	0.52
Isoleucine, %	0.96
Leucine, %	1.73
Lysine, %	1.45
Methionine, %	0.52
Cystine, %	0.37
Phenylalanine, %	0.96
Tyrosine, %	1.01
Threonine, %	0.77
Tryptophan, %	0.22
Valine, %	1.14
Alanine, %	0.55
Aspartic Acid, %	1.29
Glutamic Acid, %	4.08
Glycine, %	0.39
Proline, %	2.36
Serine, %	1.10
Taurine, %	0.00
Fat, %	***7.0***
Cholesterol, ppm	0
Linoleic Acid, %	3.58
Linolenic Acid, %	0.55
Arachidonic Acid, %	0.00
Omega-3 Fatty Acids, %	0.55
Total Saturated Fatty A	1.05
Total Monounsaturated Fatty Acids, %	1.54
Polyunsaturated Fatty Acids, %	3.78
Fiber (max), %	***30.0***
Carbohydrates, %	***38.2***
Energy (kcal/g) [2]	***2.88***

From:	kcal	%
Protein	0.721	25.0
Fat (ether extract)	0.633	22.0
Carbohydrates	1.528	53.0

Minerals	
Calcium, %	0.51
Phosphorus, %	0.32
Potassium, %	0.36
Magnesium, %	0.05
Sodium, %	0.12
Chloride, %	0.21
Fluorine, ppm	1.0
Iron, ppm	38
Zinc, ppm	35
Manganese, ppm	11
Copper, ppm	6.0
Cobalt, ppm	0.0
Iodine, ppm	0.21
Chromium (added), ppm	1.0
Molybdenum, ppm	0.14
Selenium, ppm	0.24
Vitamins	
Vitamin A, IU/g	4.0
Vitamin D-3 (added), IU/g	1.0
Vitamin E, IU/kg	81.6
Vitamin K, ppm	0.75
Thiamin, ppm	4.8
Riboflavin, ppm	6.7
Niacin, ppm	30
Pantothenic Acid, ppm	16
Folic Acid, ppm	2.1
Pyridoxine, ppm	5.8
Biotin, ppm	0.2
Vitamin B-12, mcg/kg	28
Choline Chloride, ppm	1,250
Ascorbic Acid, ppm	0.0

1. Formulation based on calculated values from the latest ingredient analysis information. Since nutrient composition of natural ingredients varies and some nutrient loss will occur due to manufacturing processes, analysis will differ accordingly. Nutrients expressed as percent of ration on an As-Fed basis except where otherwise indicated.
2. Energy (kcal/gm) - Sum of decimal fractions of protein, fat and carbohydrate x 4,9,4 kcal/gm respectively.

NOTE: When assayed, actual levels may vary from calculated values.

FSSC 22000 www.sgs.com/foodsafety SGS SYSTEM

TestDiet
www.testdiet.com

Mod TestDiet® 57W5 w/ No Cellulose, 30% Pectin 5BSX

DESCRIPTION

Modification of TestDiet® AIN-93G Semi-Purified Diet, 57W5, with no cellulose and 30% pectin.

Intended for rodents in a laboratory setting.

CAUTION: Contains a new animal drug for investigational use only in laboratory research animals or for tests in vitro. Not for use in humans.

Storage conditions are particularly critical to TestDiet® products, due to the absence of antioxidants or preservative agents. To provide maximum protection against possible changes during storage, store in a dry, cool location. Storage under refrigeration (2° C) is recommended. Maximum shelf life is six months. (If long term studies are involved, storing the diet at -20° C or colder may prolong shelf life.) Be certain to keep in air tight containers.

*Product Forms Available**	*Catalog #*
1/2" Pellet, Irradiated	1818359-203

**Other Forms Available On Request*

INGREDIENTS (%)

Pectin	30.0000
Casein - Vitamin Tested	20.0000
Corn Starch	14.7486
Maltodextrin	13.2000
Sucrose	10.0000
Soybean Oil	7.0000
AIN 93G Mineral Mix	3.5000
AIN 93G Vitamin Mix	1.0000
L-Cystine	0.3000
Choline Bitartrate	0.2500
t-Butylhydroquinone	0.0014

**See page 2 for Expanded Ingredient Listings*

FEEDING DIRECTIONS

Feed ad libitum. Plenty of fresh, clean water should be available at all times.

CAUTION:
Perishable - store properly upon receipt.
For laboratory animal use only; NOT for human consumption.

2/3/2018

NUTRITIONAL PROFILE [1]

Protein, %	***18.0***
Arginine, %	0.70
Histidine, %	0.52
Isoleucine, %	0.96
Leucine, %	1.73
Lysine, %	1.45
Methionine, %	0.52
Cystine, %	0.37
Phenylalanine, %	0.96
Tyrosine, %	1.01
Threonine, %	0.77
Tryptophan, %	0.22
Valine, %	1.14
Alanine, %	0.55
Aspartic Acid, %	1.29
Glutamic Acid, %	4.08
Glycine, %	0.39
Proline, %	2.36
Serine, %	1.10
Taurine, %	0.00
Fat, %	***7.0***
Cholesterol, ppm	0
Linoleic Acid, %	3.58
Linolenic Acid, %	0.55
Arachidonic Acid, %	0.00
Omega-3 Fatty Acids, %	0.55
Total Saturated Fatty A	1.05
Total Monounsaturated Fatty Acids, %	1.54
Polyunsaturated Fatty Acids, %	3.78
Fiber (max), %	***30.0***
Carbohydrates, %	***38.2***
Energy (kcal/g) [2]	***2.88***

From:	kcal	%
Protein	0.721	25.0
Fat (ether extract)	0.633	22.0
Carbohydrates	1.528	53.0

Minerals	
Calcium, %	0.51
Phosphorus, %	0.32
Potassium, %	0.36
Magnesium, %	0.05
Sodium, %	0.12
Chloride, %	0.21
Fluorine, ppm	1.0
Iron, ppm	38
Zinc, ppm	35
Manganese, ppm	11
Copper, ppm	6.0
Cobalt, ppm	0.0
Iodine, ppm	0.21
Chromium (added), ppm	1.0
Molybdenum, ppm	0.14
Selenium, ppm	0.24
Vitamins	
Vitamin A, IU/g	4.0
Vitamin D-3 (added), IU/g	1.0
Vitamin E, IU/kg	81.6
Vitamin K, ppm	0.75
Thiamin, ppm	4.8
Riboflavin, ppm	6.7
Niacin, ppm	30
Pantothenic Acid, ppm	16
Folic Acid, ppm	2.1
Pyridoxine, ppm	5.8
Biotin, ppm	0.2
Vitamin B-12, mcg/kg	28
Choline Chloride, ppm	1,250
Ascorbic Acid, ppm	0.0

1. Formulation based on calculated values from the latest ingredient analysis information. Since nutrient composition of natural ingredients varies and some nutrient loss will occur due to manufacturing processes, analysis will differ accordingly. Nutrients expressed as percent of ration on an As-Fed basis except where otherwise indicated.
2. Energy (kcal/gm) - Sum of decimal fractions of protein, fat and carbohydrate x 4,9,4 kcal/gm respectively.

NOTE: When assayed, actual levels may vary from calculated values.

FSSC 22000 www.sgs.com/foodsafety SGS SYSTEM

TestDiet
www.testdiet.com

Mod TestDiet® 57W5 w/ No Cellulose, 30% Inulin 5BX1

DESCRIPTION

Modification of TestDiet® AIN-93G Semi-Purified Diet, 57W5, with no cellulose and 30% inulin.

Intended for rodents in a laboratory setting.

CAUTION: Contains a new animal drug for investigational use only in laboratory research animals or for tests in vitro. Not for use in humans.

Storage conditions are particularly critical to TestDiet® products, due to the absence of antioxidants or preservative agents. To provide maximum protection against possible changes during storage, store in a dry, cool location. Storage under refrigeration (2° C) is recommended. Maximum shelf life is six months. (If long term studies are involved, storing the diet at -20° C or colder may prolong shelf life.) Be certain to keep in air tight containers.

*Product Forms Available**	*Catalog #*
1/2" Pellet, Irradiated	1818360-203

**Other Forms Available On Request*

INGREDIENTS (%)

Inulin	30.0000
Casein - Vitamin Tested	20.0000
Corn Starch	14.7486
Maltodextrin	13.2000
Sucrose	10.0000
Soybean Oil	7.0000
AIN 93G Mineral Mix	3.5000
AIN 93G Vitamin Mix	1.0000
L-Cystine	0.3000
Choline Bitartrate	0.2500
t-Butylhydroquinone	0.0014

**See page 2 for Expanded Ingredient Listings*

FEEDING DIRECTIONS

Feed ad libitum. Plenty of fresh, clean water should be available at all times.

CAUTION:
Perishable - store properly upon receipt.
For laboratory animal use only; NOT for human consumption.

2/3/2018

NUTRITIONAL PROFILE [1]

Protein, %	***18.0***
Arginine, %	0.70
Histidine, %	0.52
Isoleucine, %	0.96
Leucine, %	1.73
Lysine, %	1.45
Methionine, %	0.52
Cystine, %	0.37
Phenylalanine, %	0.96
Tyrosine, %	1.01
Threonine, %	0.77
Tryptophan, %	0.22
Valine, %	1.14
Alanine, %	0.55
Aspartic Acid, %	1.29
Glutamic Acid, %	4.08
Glycine, %	0.39
Proline, %	2.36
Serine, %	1.10
Taurine, %	0.00
Fat, %	***7.0***
Cholesterol, ppm	0
Linoleic Acid, %	3.58
Linolenic Acid, %	0.55
Arachidonic Acid, %	0.00
Omega-3 Fatty Acids, %	0.55
Total Saturated Fatty A	1.05
Total Monounsaturated Fatty Acids, %	1.54
Polyunsaturated Fatty Acids, %	3.78
Fiber (max), %	***26.4***
Carbohydrates, %	***67.0***
Energy (kcal/g) [2]	***4.03***

From:	kcal	%
Protein	0.721	17.9
Fat (ether extract)	0.633	15.7
Carbohydrates	2.680	66.4

Minerals	
Calcium, %	0.51
Phosphorus, %	0.32
Potassium, %	0.36
Magnesium, %	0.05
Sodium, %	0.14
Chloride, %	0.21
Fluorine, ppm	1.0
Iron, ppm	38
Zinc, ppm	35
Manganese, ppm	11
Copper, ppm	6.0
Cobalt, ppm	0.0
Iodine, ppm	0.21
Chromium (added), ppm	1.0
Molybdenum, ppm	0.14
Selenium, ppm	0.24
Vitamins	
Vitamin A, IU/g	4.0
Vitamin D-3 (added), IU/g	1.0
Vitamin E, IU/kg	81.6
Vitamin K, ppm	0.75
Thiamin, ppm	4.8
Riboflavin, ppm	6.7
Niacin, ppm	30
Pantothenic Acid, ppm	16
Folic Acid, ppm	2.1
Pyridoxine, ppm	5.8
Biotin, ppm	0.2
Vitamin B-12, mcg/kg	28
Choline Chloride, ppm	1,250
Ascorbic Acid, ppm	0.0

1. Formulation based on calculated values from the latest ingredient analysis information. Since nutrient composition of natural ingredients varies and some nutrient loss will occur due to manufacturing processes, analysis will differ accordingly. Nutrients expressed as percent of ration on an As-Fed basis except where otherwise indicated.
2. Energy (kcal/gm) - Sum of decimal fractions of protein, fat and carbohydrate x 4,9,4 kcal/gm respectively.

NOTE: When assayed, actual levels may vary from calculated values.

FSSC 22000 www.sgs.com/foodsafety SGS SYSTEM

TestDiet
www.testdiet.com

AIN-93G w/ 2.3% fiber from cellulose and guar gum 9GKY

DESCRIPTION

Modification of TestDiet® AIN-93G Purified Growth Diet 57W5 with 2.3% fiber. Fiber provided by equal amounts of cellulose and guar gum. Comparable to SF13-055.

CAUTION: Contains a new animal drug for investigational use only in laboratory research animals or for tests in vitro. Not for use in humans.

Storage conditions are particularly critical to TestDiet® products, due to the absence of antioxidants or preservative agents. To provide maximum protection against possible changes during storage, store in a dry, cool location. Storage under refrigeration (2° C) is recommended. Maximum shelf life is six months. (If long term studies are involved, storing the diet at -20° C or colder may prolong shelf life.) Be certain to keep in air tight containers.

Product Forms Available*	***Catalog #***
1/2" Pellet, Irradiated	1817770-203

**Other Forms Available On Request*

INGREDIENTS (%)

Corn Starch	42.4486
Casein - Vitamin Tested	20.0000
Maltodextrin	13.2000
Sucrose	10.0000
Soybean Oil	7.0000
AIN 93G Mineral Mix	3.5000
Powdered Cellulose	1.1500
Guar Gum	1.1500
AIN 93 Vitamin Mix	1.0000
L-Cystine	0.3000
Choline Bitartrate	0.2500
t-Butylhydroquinone	0.0014

FEEDING DIRECTIONS

Feed ad libitum. Plenty of fresh, clean water should be available at all times.

CAUTION:
Perishable - store properly upon receipt.
For laboratory animal use only; NOT for human consumption.

11/28/2016

NUTRITIONAL PROFILE [1]

Protein, %	***18.3***
Arginine, %	0.70
Histidine, %	0.52
Isoleucine, %	0.96
Leucine, %	1.73
Lysine, %	1.45
Methionine, %	0.52
Cystine, %	0.37
Phenylalanine, %	0.96
Tyrosine, %	1.01
Threonine, %	0.77
Tryptophan, %	0.22
Valine, %	1.14
Alanine, %	0.55
Aspartic Acid, %	1.29
Glutamic Acid, %	4.08
Glycine, %	0.39
Proline, %	2.36
Serine, %	1.10
Taurine, %	0.00
Fat, %	***7.1***
Cholesterol, ppm	0
Linoleic Acid, %	3.58
Linolenic Acid, %	0.55
Arachidonic Acid, %	0.00
Omega-3 Fatty Acids, %	0.55
Total Saturated Fatty A	1.05
Total Monounsaturated Fatty Acids, %	1.54
Polyunsaturated Fatty Acids, %	3.78
Fiber (max), %	***2.3***
Carbohydrates, %	***65.9***
Energy (kcal/g) [2]	***4.01***

From:	kcal	%
Protein	0.732	18.3
Fat (ether extract)	0.638	15.9
Carbohydrates	2.636	65.8

Minerals	
Calcium, %	0.51
Phosphorus, %	0.32
Potassium, %	0.36
Magnesium, %	0.05
Sodium, %	0.13
Chloride, %	0.22
Fluorine, ppm	1.0
Iron, ppm	39
Zinc, ppm	35
Manganese, ppm	11
Copper, ppm	6.0
Cobalt, ppm	0.0
Iodine, ppm	0.21
Chromium (added), ppm	1.0
Molybdenum, ppm	0.14
Selenium, ppm	0.24
Vitamins	
Vitamin A, IU/g	4.0
Vitamin D-3 (added), IU/g	1.0
Vitamin E, IU/kg	81.6
Vitamin K, ppm	0.75
Thiamin Hydrochloride, ppm	6.1
Riboflavin, ppm	6.7
Niacin, ppm	30
Pantothenic Acid, ppm	16
Folic Acid, ppm	2.1
Pyridoxine, ppm	5.8
Biotin, ppm	0.2
Vitamin B-12, mcg/kg	29
Choline Chloride, ppm	1,250
Ascorbic Acid, ppm	0.0

1. Formulation based on calculated values from the latest ingredient analysis information. Since nutrient composition of natural ingredients varies and some nutrient loss will occur due to manufacturing processes, analysis will differ accordingly. Nutrients expressed as percent of ration on an As-Fed basis except where otherwise indicated.
2. Energy (kcal/gm) - Sum of decimal fractions of protein, fat and carbohydrate x 4,9,4 kcal/gm respectively.

NOTE: When assayed, actual levels may vary from calculated values.

FSSC 22000

TestDiet
www.testdiet.com

AIN-93G without fiber or starch 9GKZ

DESCRIPTION

Modification of TestDiet® AIN-93G Purified Growth Diet, 57W5, with no added fiber or starch. Comparable to SF09-028.

Intended for rodents in a laboratory setting.

CAUTION: Contains a new animal drug for investigational use only in laboratory research animals or for tests in vitro. Not for use in humans.

Storage conditions are particularly critical to TestDiet® products, due to the absence of antioxidants or preservative agents. To provide maximum protection against possible changes during storage, store in a dry, cool location. Storage under refrigeration (2° C) is recommended. Maximum shelf life is six months. (If long term studies are involved, storing the diet at -20° C or colder may prolong shelf life.) Be certain to keep in air tight containers.

*Product Forms Available**	*Catalog #*
1/2" Pellet, Irradiated	1817771-203

**Other Forms Available On Request*

INGREDIENTS (%)

Dextrose	67.9486
Casein - Vitamin Tested	20.0000
Soybean Oil	7.0000
AIN 93G Mineral Mix	3.5000
AIN 93 Vitamin Mix	1.0000
L-Cystine	0.3000
Choline Bitartrate	0.2500
t-Butylhydroquinone	0.0014

**See page 2 for Expanded Ingredient Listings*

FEEDING DIRECTIONS

Feed ad libitum. Plenty of fresh, clean water should be available at all times.

CAUTION:
Perishable - store properly upon receipt.
For laboratory animal use only; NOT for human consumption.

5/2/2017

NUTRITIONAL PROFILE [1]

Protein, %	***17.9***
Arginine, %	0.70
Histidine, %	0.52
Isoleucine, %	0.96
Leucine, %	1.73
Lysine, %	1.45
Methionine, %	0.52
Cystine, %	0.37
Phenylalanine, %	0.96
Tyrosine, %	1.01
Threonine, %	0.77
Tryptophan, %	0.22
Valine, %	1.14
Alanine, %	0.55
Aspartic Acid, %	1.29
Glutamic Acid, %	4.08
Glycine, %	0.39
Proline, %	2.36
Serine, %	1.10
Taurine, %	0.00
Fat, %	***7.0***
Cholesterol, ppm	0
Linoleic Acid, %	3.58
Linolenic Acid, %	0.55
Arachidonic Acid, %	0.00
Omega-3 Fatty Acids, %	0.55
Total Saturated Fatty A	1.05
Total Monounsaturated Fatty Acids, %	1.54
Polyunsaturated Fatty Acids, %	3.78
Fiber (max), %	***0.0***
Carbohydrates, %	***68.9***
Energy (kcal/g) [2]	***4.10***

From:	kcal	%
Protein	0.715	17.4
Fat (ether extract)	0.630	15.4
Carbohydrates	2.757	67.2

Minerals	
Calcium, %	0.50
Phosphorus, %	0.32
Potassium, %	0.36
Magnesium, %	0.05
Sodium, %	0.11
Chloride, %	0.17
Fluorine, ppm	1.0
Iron, ppm	37
Zinc, ppm	35
Manganese, ppm	11
Copper, ppm	6.0
Cobalt, ppm	0.0
Iodine, ppm	0.21
Chromium (added), ppm	1.0
Molybdenum, ppm	0.14
Selenium, ppm	0.24

Vitamins	
Vitamin A, IU/g	4.0
Vitamin D-3 (added), IU/g	1.0
Vitamin E, IU/kg	81.6
Vitamin K, ppm	0.75
Thiamin Hydrochloride, ppm	4.8
Riboflavin, ppm	6.7
Niacin, ppm	30
Pantothenic Acid, ppm	16
Folic Acid, ppm	2.1
Pyridoxine, ppm	5.8
Biotin, ppm	0.2
Vitamin B-12, mcg/kg	28
Choline Chloride, ppm	1,250
Ascorbic Acid, ppm	0.0

1. Formulation based on calculated values from the latest ingredient analysis information. Since nutrient composition of natural ingredients varies and some nutrient loss will occur due to manufacturing processes, analysis will differ accordingly. Nutrients expressed as percent of ration on an As-Fed basis except where otherwise indicated.
2. Energy (kcal/gm) - Sum of decimal fractions of protein, fat and carbohydrate x 4,9,4 kcal/gm respectively.

NOTE: When assayed, actual levels may vary from calculated values.

FSSC 22000 www.sgs.com/foodsafety SGS SYSTEM

TestDiet
www.testdiet.com

AIN-93G Growth Purified Diet (also known as #5801-G) 57W5

DESCRIPTION

TestDiet® AIN-93G Growth Purified Diet is the growth diet for rodents recommended by the American Institute of Nutrition. It is formulated to substitute for the previous version (AIN-76A) to improve animal performance.

CAUTION: Contains a drug or compound for investigational use only in laboratory research animals or in vitro. Not for human use.

Storage conditions are particularly critical to TestDiet® products, due to the absence of antioxidants or preservative agents. To provide maximum protection against possible changes during storage, store in a dry, cool location. Storage under refrigeration (2° C) is recommended. Maximum shelf life is six months. (If long term studies are involved, storing the diet at -20° C or colder may prolong shelf life.) Be certain to keep in air tight containers.

*Product Forms Available**	*Catalog #*
1/2" Pellet	7597
1/2" Pellet, Irradiated	1810393
1/2" Pellet, Irradiated, 5 Kg Heat Seal	1816530
Meal	1810538

**Other Forms Available On Request*

INGREDIENTS (%)

Corn Starch	39.7486
Casein - Vitamin Tested	20.0000
Maltodextrin	13.2000
Sucrose	10.0000
Soybean Oil	7.0000
Powdered Cellulose	5.0000
AIN 93G Mineral Mix	3.5000
AIN 93 Vitamin Mix	1.0000
L-Cystine	0.3000
Choline Bitartrate	0.2500
t-Butylhydroquinone	0.0014

FEEDING DIRECTIONS

Feed ad libitum to mice and rats. Plenty of fresh, clean water should be available at all times.

CAUTION:
Perishable - store properly upon receipt.
For laboratory animal use only; NOT for human consumption.

11/18/2014

NUTRITIONAL PROFILE [1]

Protein, %	***18.3***
Arginine, %	0.70
Histidine, %	0.52
Isoleucine, %	0.96
Leucine, %	1.73
Lysine, %	1.45
Methionine, %	0.52
Cystine, %	0.37
Phenylalanine, %	0.96
Tyrosine, %	1.01
Threonine, %	0.77
Tryptophan, %	0.22
Valine, %	1.14
Alanine, %	0.55
Aspartic Acid, %	1.29
Glutamic Acid, %	4.08
Glycine, %	0.39
Proline, %	2.36
Serine, %	1.10
Taurine, %	0.00
Fat, %	***7.1***
Cholesterol, ppm	0
Linoleic Acid, %	3.58
Linolenic Acid, %	0.55
Arachidonic Acid, %	0.00
Omega-3 Fatty Acids, %	0.55
Total Saturated Fatty A	1.05
Total Monounsaturated Fatty Acids, %	1.54
Polyunsaturated Fatty Acids, %	3.78
Fiber (max), %	***5.0***
Carbohydrates, %	***63.2***
Energy (kcal/g) [2]	***3.90***

From:	kcal	%
Protein	0.731	18.8
Fat (ether extract)	0.637	16.4
Carbohydrates	2.528	64.9

Minerals	
Calcium, %	0.51
Phosphorus, %	0.32
Potassium, %	0.36
Magnesium, %	0.05
Sodium, %	0.13
Chloride, %	0.22
Fluorine, ppm	1.0
Iron, ppm	40
Zinc, ppm	35
Manganese, ppm	11
Copper, ppm	6.0
Cobalt, ppm	0.0
Iodine, ppm	0.21
Chromium (added), ppm	1.0
Molybdenum, ppm	0.14
Selenium, ppm	0.24
Vitamins	
Vitamin A, IU/g	4.0
Vitamin D-3 (added), IU/g	1.0
Vitamin E, IU/kg	81.6
Vitamin K, ppm	0.75
Thiamin Hydrochloride, ppm	6.1
Riboflavin, ppm	6.7
Niacin, ppm	30
Pantothenic Acid, ppm	16
Folic Acid, ppm	2.1
Pyridoxine, ppm	5.8
Biotin, ppm	0.2
Vitamin B-12, mcg/kg	29
Choline Chloride, ppm	1,250
Ascorbic Acid, ppm	0.0

1. Formulation based on calculated values from the latest ingredient analysis information. Since nutrient composition of natural ingredients varies and some nutrient loss will occur due to manufacturing processes, analysis will differ accordingly. Nutrients expressed as percent of ration on an As-Fed basis except where otherwise indicated.
2. Energy (kcal/gm) - Sum of decimal fractions of protein, fat and carbohydrate x 4,9,4 kcal/gm respectively.

ISO 9001:2008 CERTIFIED

TestDiet
www.testdiet.com

Mod TestDiet® AIN-93G w/ 5% Fiber from Cellulose & Guar Gu 9GQP

DESCRIPTION

Modification of TestDiet® AIN-93G Semi-Purified Diet, 57W5, with 5% Fiber (50% from cellulose and 50% from guar gum).

Intended for rodents in a laboratory setting.

CAUTION: Contains a new animal drug for investigational use only in laboratory research animals or for tests in vitro. Not for use in humans.

Storage conditions are particularly critical to TestDiet® products, due to the absence of antioxidants or preservative agents. To provide maximum protection against possible changes during storage, store in a dry, cool location. Storage under refrigeration (2° C) is recommended. Maximum shelf life is six months. (If long term studies are involved, storing the diet at -20° C or colder may prolong shelf life.) Be certain to keep in air tight containers.

Product Forms Available*	***Catalog #***
1/2" Pellet, Irradiated	1818039-203

**Other Forms Available On Request*

INGREDIENTS (%)

Corn Starch	39.7486
Casein - Vitamin Tested	20.0000
Maltodextrin	13.2000
Sucrose	10.0000
Soybean Oil	7.0000
AIN 93G Mineral Mix	3.5000
Powdered Cellulose	2.5000
Guar Gum	2.5000
AIN 93 Vitamin Mix	1.0000
L-Cystine	0.3000
Choline Bitartrate	0.2500
t-Butylhydroquinone	0.0014

**See page 2 for Expanded Ingredient Listings*

FEEDING DIRECTIONS

Feed ad libitum. Plenty of fresh, clean water should be available at all times.

CAUTION:
Perishable - store properly upon receipt.
For laboratory animal use only; NOT for human consumption.

4/12/2017

NUTRITIONAL PROFILE [1]

Protein, %	***18.3***
Arginine, %	0.70
Histidine, %	0.52
Isoleucine, %	0.96
Leucine, %	1.73
Lysine, %	1.45
Methionine, %	0.52
Cystine, %	0.37
Phenylalanine, %	0.96
Tyrosine, %	1.01
Threonine, %	0.77
Tryptophan, %	0.22
Valine, %	1.14
Alanine, %	0.55
Aspartic Acid, %	1.29
Glutamic Acid, %	4.08
Glycine, %	0.39
Proline, %	2.36
Serine, %	1.10
Taurine, %	0.00
Fat, %	***7.1***
Cholesterol, ppm	0
Linoleic Acid, %	3.58
Linolenic Acid, %	0.55
Arachidonic Acid, %	0.00
Omega-3 Fatty Acids, %	0.55
Total Saturated Fatty A	1.05
Total Monounsaturated Fatty Acids, %	1.54
Polyunsaturated Fatty Acids, %	3.78
Fiber (max), %	***5.0***
Carbohydrates, %	***63.2***
Energy (kcal/g) [2]	***3.90***

From:	**kcal**	**%**
Protein	0.731	18.8
Fat (ether extract)	0.637	16.4
Carbohydrates	2.528	64.9

Minerals	
Calcium, %	0.51
Phosphorus, %	0.32
Potassium, %	0.36
Magnesium, %	0.05
Sodium, %	0.13
Chloride, %	0.22
Fluorine, ppm	1.0
Iron, ppm	39
Zinc, ppm	35
Manganese, ppm	11
Copper, ppm	6.0
Cobalt, ppm	0.0
Iodine, ppm	0.21
Chromium (added), ppm	1.0
Molybdenum, ppm	0.14
Selenium, ppm	0.24
Vitamins	
Vitamin A, IU/g	4.0
Vitamin D-3 (added), IU/g	1.0
Vitamin E, IU/kg	81.6
Vitamin K, ppm	0.75
Thiamin Hydrochloride, ppm	4.8
Riboflavin, ppm	6.7
Niacin, ppm	30
Pantothenic Acid, ppm	16
Folic Acid, ppm	2.1
Pyridoxine, ppm	5.8
Biotin, ppm	0.2
Vitamin B-12, mcg/kg	28
Choline Chloride, ppm	1,250
Ascorbic Acid, ppm	0.0

1. Formulation based on calculated values from the latest ingredient analysis information. Since nutrient composition of natural ingredients varies and some nutrient loss will occur due to manufacturing processes, analysis will differ accordingly. Nutrients expressed as percent of ration on an As-Fed basis except where otherwise indicated.
2. Energy (kcal/gm) - Sum of decimal fractions of protein, fat and carbohydrate x 4,9,4 kcal/gm respectively.

NOTE: When assayed, actual levels may vary from calculated values.

FSSC 22000
www.sgs.com/foodsafety

TestDiet
www.testdiet.com